TRANSITIONS IN CHROMIUM

Thesis by

Jean-François Marin

In Partial Fulfillment of the Requirements

For the Degree of

Doctor of Philosophy

California Institute of Technology

Pasadena, California

ACKNOWLEDGEMENTS

The writer wishes to express his deep gratitude to Professor Pol Duwez for his encouragement and advice during the course of this investigation. He is also indebted to Dr. E. Stern for the use of his equipment for elastic constants determinations and to Mr. R. Willens for many helpful suggestions. Messrs. M. Malcolm and R. Lallement provided valuable assistance in the elastic constants measurements; Mr. S. Chow prepared tracings for most of the figures; Mrs. R. Mercer typed the manuscript. Gratitude is due to the Office of Naval Research and the U.S. Atomic Energy Commission for their combined support of this study.

ABSTRACT

The presence of a transition in pure chromium around 40C (from 25C to 65C according to the specimen investigated) is evidenced by the anomalous behavior of various physical properties in the vicinity of the transition. Four different properties - electrical resistivity, Young's modulus and Poisson's ratio, Hall coefficient, specific heat - have been investigated on some of five different specimens in temperature ranges including the transition temperature.

The shape and magnitude of the observed anomalies for different properties and different specimens are compared, together with the possible effect of impurities on the transition. The relationship between these anomalies and the transition from an antiferromagnetic to a paramagnetic structure is discussed in connection with neutron diffraction experiments and anomalies in other antiferromagnetic materials reported by other workers.

TABLE OF CONTENTS

LIST OF FIGURES AND TABLES

I INTRODUCTION

Some metals and many alloys undergo phase transitions under some critical conditions of temperature and pressure. These transitions are usually classified into two broad groups. The first group refers to the so-called first order transitions, in which crystal structure, energy and volume change discontinuously. The second group includes the second - or higher - order transitions (also referred to as continuous transitions or λ-points); in this type of transition, the energy and volume change continuously, but the temperature derivatives of these quantities, i.e. specific heat and expansion coefficient, in general exhibit discontinuities.

The mechanism of the transitions of the first kind and the corresponding crystal structure change have been successfully investigated for most metals and many multicomponent alloys; in this case, X-ray studies always provide direct and detailed information about the geometry of the lattice and the energy discontinuity between the two phases can be directly measured. In a continuous transition, the solid generally undergoes a change in atomic ordering within the crystal lattice, or a change in properties such as ferromagnetism, ferroelectricity, superconductivity, etc. These phenomena sometimes lend themselves to direct investigation: order-disorder transformations in alloys can be studied by X-ray diffraction, magnetic order - disorder transformations require neutron diffraction techniques. In some cases, however, these transitions have been discovered, investigated or even defined by the measurement of some indirect property whose variation under the critical conditions is most characteristic. The existence of transitions in pure chromium has been observed by several authors

in recent years. These transitions were detected in measurements of electrical resistivity[1-3], thermoelectric power[2-3], thermal expansivity[4-5], paramagnetic susceptibility[6-7], Young's modulus[8-10], lattice constant and internal friction[8].

All the published experimental results exhibited some remarkable features, but suggested no simple clue for a possible explanation of the transition; moreover, the results of different authors showed rather large discrepancies that could be ascribed either to differences in the techniques used or to the purity and processing of the specimens under investigation. The present work was undertaken in an effort to explain some of the inconsistencies in the published data. The electrical resistivity, Young's modulus, Hall coefficient, magnetoresistance coefficient and specific heat have been investigated. The results reported in this thesis, together with recent works of other authors strongly suggest that the transition in chromium is closely related to the change from a paramagnetic to an antiferromagnetic state.

II REVIEW OF PREVIOUS WORK

An anomalous temperature dependence of the physical properties of pure chromium was reported for the first time by Bridgman[1], in the course of an investigation of the influence of pressure on the electrical resistance of various elements. In the case of chromium, he found that the temperature coefficient of resistance at atmospheric pressure becomes negative between about -5 C and + 10 C. He also established that an increase in pressure depresses the temperature of this anomaly and lowers the absolute value of the resistivity; the temperature of the minimum in resistivity changes from 12 C at atmospheric pressure down to about -50C at 8×10^3 kgm/cm^2. A few years later, Söchtig[2] and Potter[3] independently correlated the anomaly in resistivity with an anomaly in thermoelectric power at the same temperature, around 38 C in both investigations. Potter studied also the influence of annealing: while the resistivity decreases when annealing is carried out for a longer time or at higher temperature, the shape of the resistivity versus temperature curve and the temperature of the transition do not change. Söchtig investigated some impure samples, and the transition was found to take place at lower temperatures and over a much larger range of temperature. He did not find any anomaly in the magnetic susceptibility nor any detectable heat of transformation when the specimen was cooled slowly through the transition region.

At the same time, Erfling[4] and Hidnert[5] found anomalies in the thermal expansivity versus temperature curves. While Erfling reported a smooth decrease of the coefficient between -10C and +30C,

Hidnert found a sharp minimum for the two specimens he investigated. Additional results reported by Bates and Baqi[6] and by McGuire and Kriessman[7] indicate that the transition has no detectable effect on the paramagnetic susceptibility.

More recently, the study of the temperature dependence of the elastic constants has disclosed quite remarkable features. Fine, Greiner and Ellis[8], using electronic methods for determining resonance frequencies, found a sharp drop of about 4% in Young's modulus at 37 C; they detected also a similar anomaly of much smaller magnitude at -151 C. They investigated a number of other physical properties on the two same specimens, one pressed electrolytic sample and one electroformed sample: they confirmed the anomalies in electrical resistivity, thermoelectric power, coefficient of expansion and, in addition, found a sharp peak in internal friction; the variation of the lattice constant in the range of temperature 0 to 60 C was studied by X-ray diffraction (powder method) and did not disclose any departure from linearity in the transition region. In all cases where an anomaly was found in a physical property, it was observed at 37 C. However, the low temperature anomaly at -151 C was observed only in Young's modulus. Using a resonance frequency technique, Pursey[9] confirmed the anomaly at 37 C in the elastic constants, on an electroformed sample with 1.6% impurities, annealed at 540 C for 15 hours. He computed the variation of Poisson's ratio in the transition region and studied[10] the dependence of Young's modulus on the frequency of the vibrations.

Contrary to the results of Fine et al[8], Straumanis and Weng[11]

observed a break in the lattice parameter versus temperature curve, between two regions where the lattice constant varies linearly; the expansion coefficient is 4.4×10^{-6} $(C)^{-1}$ in the lower range, $7.47 \times 10^{-6}(C)^{-1}$ in the upper range, and the break occurs at 32.5 C.

In neutron diffraction studies of a chromium powder sample, Shull and Wilkinson[12] investigated the intensity of the (100) antiferromagnetic reflection as a function of temperature. They concluded that chromium is weakly antiferromagnetic, with an effective magnetic moment of 0.4 Bohr magneton per atom and a Néel temperature of about 200 C. More recent experiments on single crystals, by Weiss et al[13] and Bykov et al[14] confirmed the antiferromagnetic structure, but indicated a Néel temperature around 40 C.

Various hypotheses concerning the nature of the transition were suggested by some of the authors mentioned above. The anomaly in thermal expansivity[4,5,8] pointed to a crystal structure change, which was contradicted, however, by X-ray diffraction experiments[8,11]. As pointed out by Söchtig[2], the anomaly in electrical resistivity could be accounted for by a change in the proportion of 4s to 3d electrons, which belong to overlapping bands in chromium; the rather peculiar electronic configuration of the ground state of the chromium atom ($3d^5$ $4s^1$) should be noted here, which makes chromium the only element in the first transition group with an incomplete s-shell. An electronic transition of this kind can in turn be related to a critical change in the interatomic forces to explain the large volume effect occuring during the transition. Indeed, using thermal expansivity results[4,5,8] and the pressure dependence of the anomaly[1], Fine,

Greiner, Ellis[8] and Pursey[15] found convenient to describe the transition as an anomalous volume contraction of the order of 6×10^{-4} in^3 per in^3 upon heating through the transition. Such contraction would cause the additional strain which accounts for the observed initial drop in Young's modulus and the minimum in Poisson's ratio.

Finally, the determination of the Néel temperature of single crystals allowed Weiss[13] and Bykov[14] to relate the transition to the loss of antiferromagnetism; the similarity of the anomalies in chromium with those exhibited by other antiferromagnetic materials at their Néel point had already been pointed out[8,15].

Additional experimental data and more particular aspects of the transition are discussed in Part 6.

III SPECIMENS

The characteristics (origin, dimensions, purity, history) of the samples which have been investigated and the various experiments performed on each of them are reported in Table I.

ORIGIN AND NOMENCLATURE	SHAPE AND DIMENSIONS	PURITY	HISTORY	EXPERIMENTS PERFORMED
Bureau of Mines BM I	Rod 2.5 x 0.25 in	Al < 0.1% Cu < 0.01% Fe < 0.1% Si < 0.1%	Annealed 2 hours at 750 C	YM
Bureau of Mines BM II & BM II'	Rod 2.5 x 0.25 in		As received (BM II) & annealed 2 hours at 900 C (BM II')	R , YM
Bureau of Mines BM III	Strip 5.5 x 0.41 x 0.032 in	O < 200 ppm H < 5 ppm N < 50 ppm	Annealed 2 hours at 900 C	R
Watertown Arsenal WI	Rod 2.5 x 0.25 in	Unspecified	Annealed 2 hours at 900 C	R , YM , HE
Batelle Institute BT	Strip 3.5 x 0.44 x 0.062 in	0.006% O 0.002% N 0.008% C total metallic impurities less than 0.005%	Annealed 2 hours at 900 C	R , HE
Wright Air Center WR	Rod 2.5 x 0.25 in	Unspecified	As received	R , SH

The following abbreviations have been used in this Table:

R for Resistivity
YM for Young's modulus
HE for Hall effect
SH for Specific heat

TABLE I

IV EXPERIMENTAL AND CALCULATION METHODS

4.1. RESISTIVITY .

The electrical resistivity of five samples has been investigated in the range of temperature from liquid nitrogen to 135 C. The specimens were received in the form of strips and rods whose dimensions are indicated in Table I. Because of the brittleness of chromium, these specimens could not be further reduced in dimensions and the resistivity measurements were handicapped by the low resistance of the samples (from about 200 $\mu\Omega$ to 2000 $\mu\Omega$ at room temperature).

4.1.1. Principle of Bridge Measurements.

For accurate measurements of low electrical resistance, the Kelvin Bridge method is most suitable. As in a Wheatstone Bridge, the unknown resistance is connected in one branch of a circuit, and a calibrated resistance in another branch is adjusted until a galvanometer in a diagonal arm shows that the circuit is electrically balanced. In a Kelvin Bridge, in order to minimize the effect of the resistance of leads and contacts of the unknown resistance, high resistances (a few hundred ohms) are inserted in series with the specimen leads. This circuit requires the use of distinct current and potential terminals for both the standard and the unknown resistance. A schematic diagram of the circuit is shown in Fig. 1.

4.1.2. Experimental Technique.

Fig. 2 shows the main features of the experimental arrangement used in resistance studies. The specimens are either small rods or strips with the dimensions indicated in Table I. For each type of

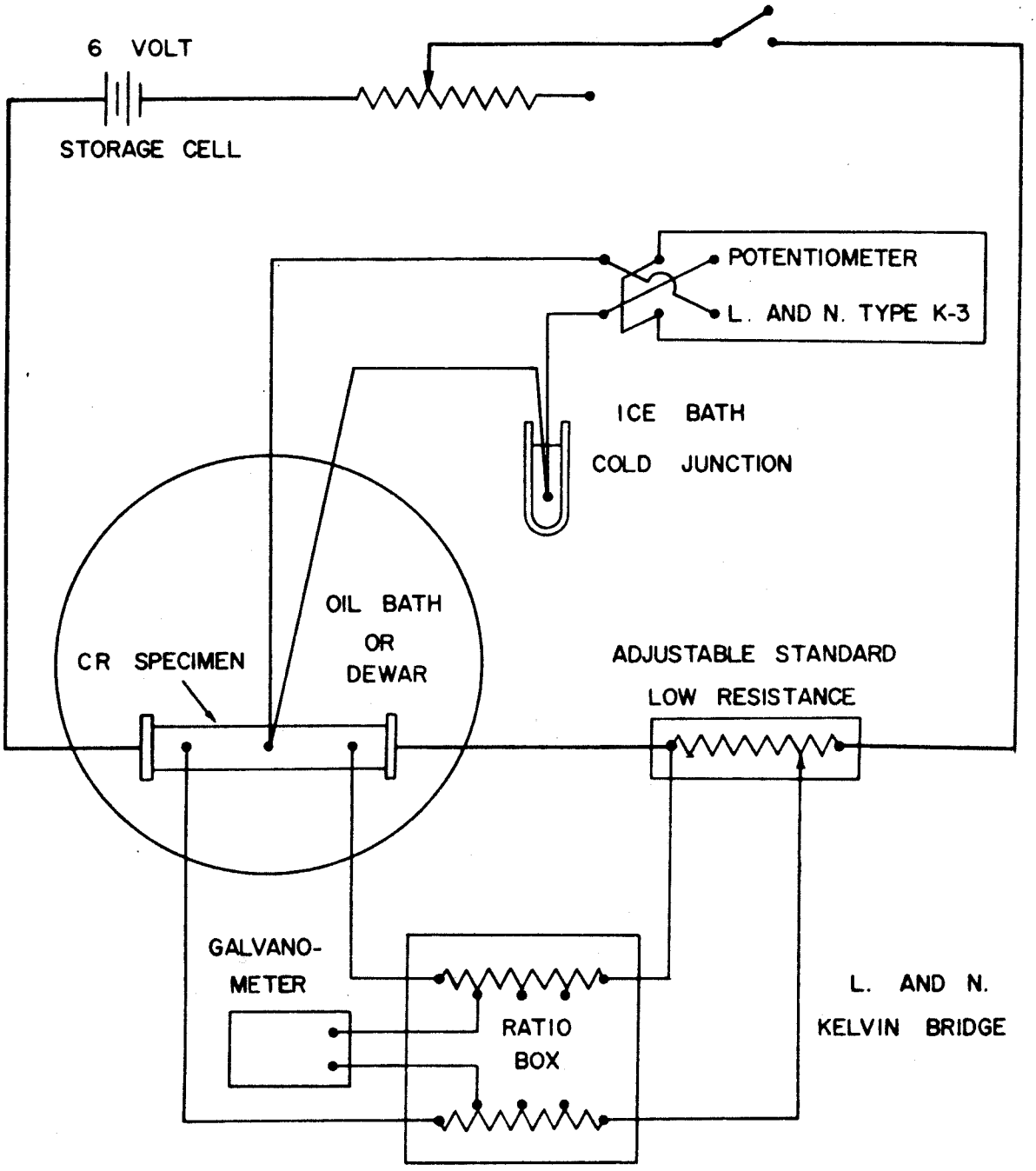

Fig. 1. Schematic diagram of resistance measurements.

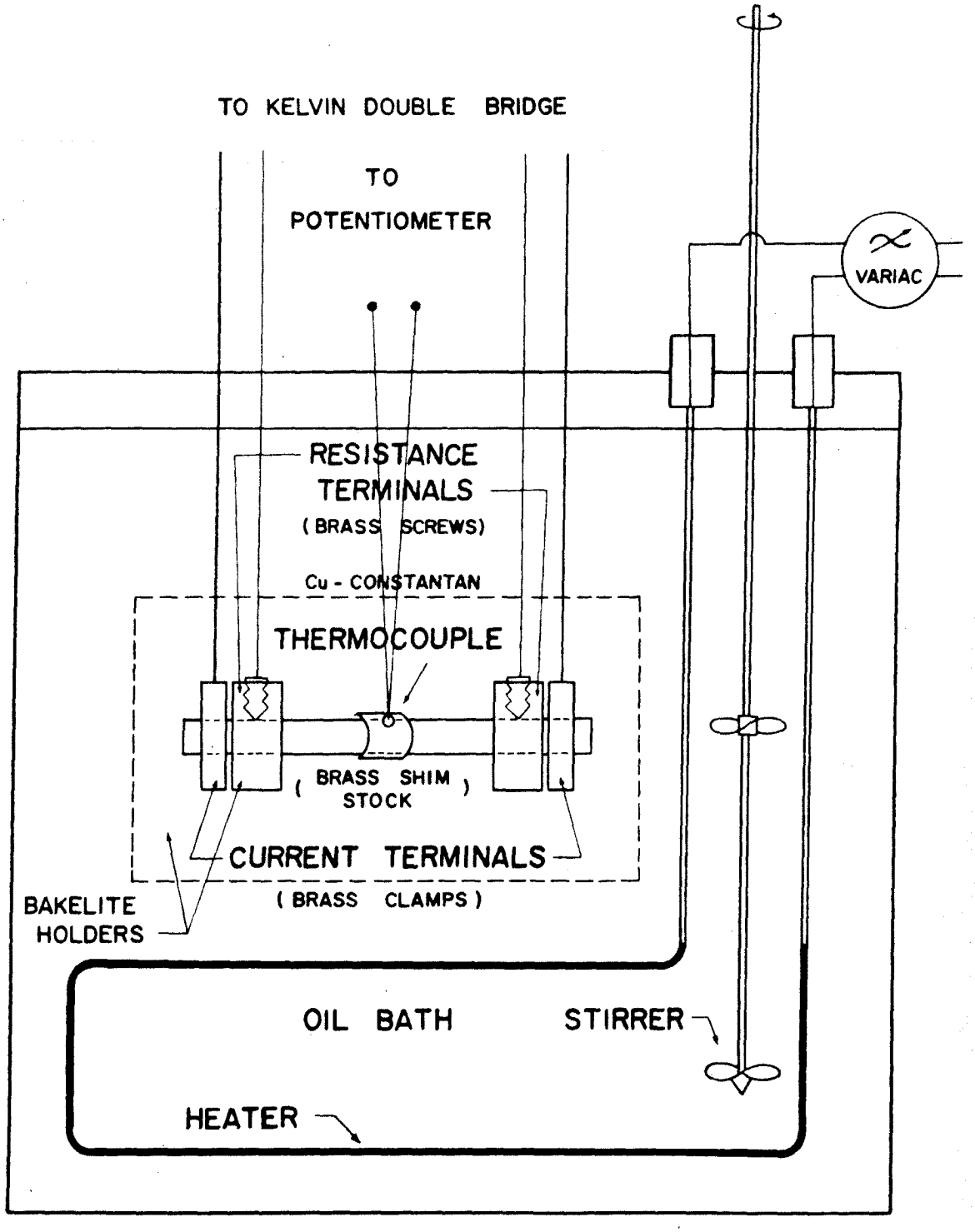

Fig. 2. Sketch of the oil bath for resistance measurements above room temperature.

specimen, a special bakelite holder was made for fixed positioning of the various electrical leads to the specimen.

Current terminals - They bring the main current through the specimen and consist in brass pressure clamps, about 1 x 1/4 x 1/4 in., machined either with a narrow slot for strips or a small cylindrical hole for rods; the two halves of the clamp are screwed together to fit tightly to the specimen and exert enough pressure to insure good electrical contact.

Potential terminals - They limit the part of the specimen whose resistance is actually measured; they consist of small brass screws inserted in a bakelite holder, making a sharp point contact with the specimen. A copper wire is soldered to the other end of the screw, leading to the Ratio Box of the Kelvin Bridge.

Thermocouple - One junction of a Copper-Constantan thermocouple is soldered to a piece of brass stock held in close contact around the center part of the specimen by a small bakelite piece. These various holders and clamps are held rigidly together by a larger adjustable bakelite holder, which releases any strain the other attachments might exert on the specimen and insulates electrically the complete setup from the brass walls of the oil bath.

Oil bath - Isothermal conditions above room temperature are obtained by immersing the specimen in an oil bath. Its shape and dimensions are designed to meet also the requirements for Hall and magnetoresistance coefficients measurements. Essentially, a compromise has to be made between the minimum volume of oil to be used, the minimum room necessary for the specimen and its attachments, on

one hand, and the maximum air gap between the poles of the magnet, on the other hand. The bath is a thin parallelepipedic box 12 x 13 x 3/4 in., made of brass and covered with several layers of asbestos paper in order to minimize heat losses. The total thickness of the bath is a little less than 7/8 in., which is the gap width used in the magnetic experiments.

A range of temperatures between room temperature and + 135 C is obtained using a Tube type immersion heater, with a power of 125 w, a heating length of 32 in. on a total length of 48 in., and bent as shown in Fig. 2. In order to obtain a stable constant temperature in the bath, a Microset regulator was first used; however, because of the lack of space, the regulator could not be kept close enough to the specimen and this type of regulation gave a sawtooth variation of temperature in the vicinity of the specimen. A much better stability is obtained through the use of a constant power input to the heater; any voltage up to 130 V can be applied to the heating resistor by means of a "Variac" transformer, by increments small enough to produce a variation of the bath temperature of less than one tenth of a degree; by letting the system reach equilibrium, which can require as long as one hour, a very stable temperature is attained. Finally, in order to get a temperature as uniform as possible throughout the bath, the oil is stirred by two small nylon propellers mounted on a brass rod rotating at high speed (1750 rpm).

For investigations in the low temperature range, from liquid nitrogen temperature (-195 C) to room temperature, the specimen is placed in a 3 ft. high Dewar vessel, a few inches above the bottom

where liquid nitrogen is boiled. After the liquid nitrogen has been completely evaporated, the system goes slowly back to room temperature, in about one and a half days.

4.1.3. Operation and accuracy.

As mentioned in "Principle of Bridge measurements", the standard resistance is adjusted until the circuit is electrically balanced, once the proper arm ratio has been chosen. This choice is made so that the fullest advantage is taken of the accuracy of the 10,100 microohms standard resistance; four significant figures can be read (i.e., to 1 $\mu\Omega$), and by interpolation on the vernier scale, 0.1 $\mu\Omega$ can be estimated. Readings can be made with a sensitivity of 0.01 per cent for the specimens having a resistance as low as a few microohms.

The thermal emf of the copper constantan thermocouple in contact with the specimen is measured by a Leeds & Northrup K3 potentiometer; the sensitivity is better than 1 μV, which corresponds, at room temperature, to about two hundredths of one degree. More important factors of uncertainties are the lack of uniformity of the temperature within the bath at any given time and the time dependent drift in the bath temperature at any one location. The fact that these two factors are of importance is evidenced by the following observations: 1) A small thermal emf was observed between the potential terminals which act as a brass-chromium thermocouple. 2) A small hysteresis was observed (Fig. 12 and 13) between heating and cooling experiments, only when the bath had not reached equilibrium. Whenever sufficient

time was allowed for the bath to reach its equilibrium temperature, there was complete agreement between results obtained during heating or cooling.

4.1.4. Resistivity conversion.

Although the resistance measurements are obtained with relatively high accuracy, there is some uncertainty in converting these data into resistivity results. One reason is the difficulty in measuring the dimensions of the sample; because chromium cannot be machined easily, the dimensions and especially the thickness of the sheet specimen are not uniform. Another source of error in the resistivity data is the uncertainty in the measurement of the distance between the two contact probes.

For a strip of thickness t, width W, resistance R between probes a length l apart, the uncertainty on the resistivity may be expressed by:

$$\frac{\Delta\rho}{\rho} = \frac{\Delta R}{R} + \frac{\Delta t}{t} + \frac{\Delta W}{W} + \frac{\Delta l}{l} \qquad (4.1)$$

For a rod of diameter d, resistance R between probes distant by l, the uncertainty is:

$$\frac{\Delta\rho}{\rho} = \frac{\Delta R}{R} + \frac{\Delta l}{l} + 2\frac{\Delta d}{d} \qquad (4.2)$$

For a strip, it is estimated that $\frac{\Delta R}{R} = 0.01\%$, $\frac{\Delta t}{t} = 3\%$, $\frac{\Delta W}{W} = 0.5\%$ $\frac{\Delta l}{l} = 3\%$. This leads to a total uncertainty of the order of 7% on ρ. For a rod, $\frac{\Delta R}{R} = 0.01\%$, $\frac{\Delta l}{l} = 5\%$, $\frac{\Delta d}{d} = 0.5\%$ and the total uncertainty is of the order of 6%.

4.2. YOUNG'S MODULUS AND POISSON'S RATIO

4.2.1. Experimental technique.

The method provides measurements of the longitudinal resonant frequencies of cylindrical specimens, from which dynamic elastic constants (Young's modulus E, Poisson's ratio σ) are derived. To excite a specimen into longitudinal vibrations, an electrostatic method is used(*). The specimen is driven from an oscillator by the electrostatic force due to an alternating voltage applied to the condenser constituted by the end of a driver and one end of the specimen. The detection of the resonance is carried out at the same end of the specimen, the capacitance between the driver and the specimen being the capacitance of a 60 MC/s oscillator, which is frequency modulated by the vibration of the specimen. This frequency modulated signal is converted into an amplitude modulated signal and fed into a detector; its output is then at the drive frequency and has an amplitude proportional to the amplitude of vibration of the specimen. The operation is a simple adjustment of the drive frequency corresponding to the maximum of amplitude vibration. The main features of the circuit are shown in Fig. 3.

The method requires specimens in the shape of cylinders of approximately 2.5 in. long and 0.25 in. in diameter. The specimen is held by three sharp points in its center, which is thus a node for all vibrations. The driving electrode, also 0.25 in. diameter, is kept closely parallel, opposite the end of the specimen; it can be adjusted

* This equipment was built by Edward A. Stern at the California Institute in 1957.

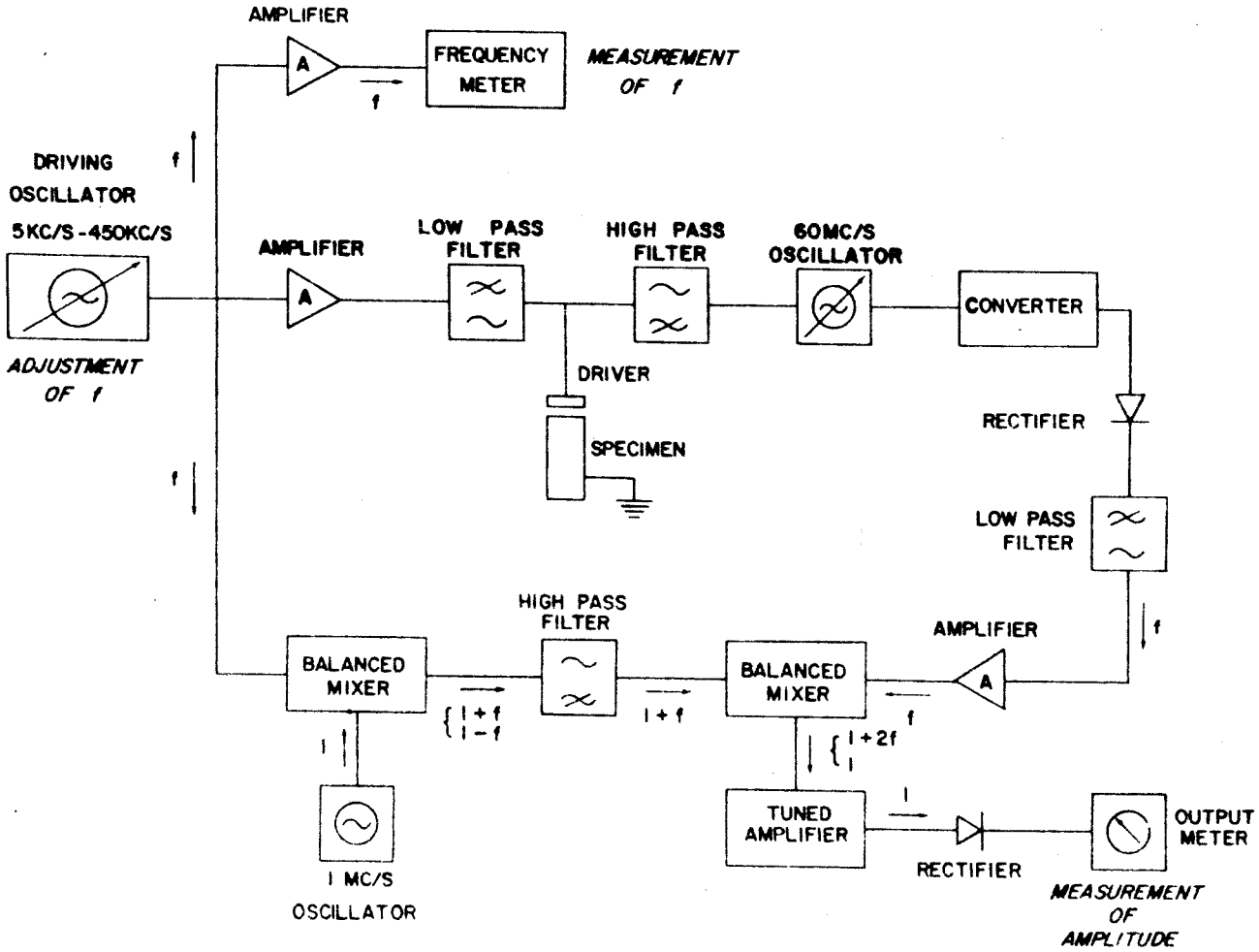

Fig. 3. Block diagram of the circuit for resonant frequencies determination.

by a differential screw to make a gap of the order of 0.001 in. Both specimen and driver are mounted and enclosed in a long insulated holder, allowing immersion in a constant temperature bath.

The driving oscillator is a Hewlett Packard Wide-range oscillator Model 200 CD; it covers a range from 5 to 600 KC/s in five overlapping bands; a range from about 50 KC/s (corresponding to the first mode) to 500 KC/s is used in this investigation. This frequency is measured on a Berkeley Universal EPUT and Timer Model 7360, within a few parts in several ten thousands.

Isothermal conditions between liquid nitrogen temperature and room temperature are obtained by placing the specimen and its holder in a deep Dewar vessel which heats up slowly after some nitrogen has been boiled at the bottom. For experiments between room temperature and 100 C, the holder is immersed in a water bath, a large aluminum container with 30 gallons of water and styrofoam insulation around it; the bath is heated with a 2000 W Tube type immersion heater. A constant power input is provided to the heater by applying any voltage up to 130 V by means of a Variac transformer. In order to insure good temperature uniformity throughout the bath, the water is stirred by a 2 in. propeller mounted on a fast rotating shaft.

Since it is impossible to keep a thermocouple in contact with the specimen during the operation, two Copper-Constantan thermocouples are mounted in contact with the holder, in the region of the specimen, one inside, one outside the holder; these two readings also indicate how close the system is to thermal equilibrium. In the high temperature range, the "inside" thermocouple is mounted on a small bakelite holder

kept close to the lower end of the specimen.

Temperature readings are performed both before and after frequency determinations, in order to check for a possible temperature drift of the bath (or of the Dewar atmosphere). At each temperature, the frequencies corresponding to various modes are determined by a resonance method. The frequency corresponding to the first mode is approximately computed, then experimentally determined. Since the low-mode peaks are very sharp, the range of frequencies of interest is scanned very slowly. Once the first mode has been determined, the higher modes, up to number 11 or 13, are determined without ambiguity.

The length L, the diameter d, and the mass m of the specimen are also measured at room temperature, the length within $\pm$ 0.02%, the diameter within $\pm$ 0.1%, the mass within $\pm$ 0.005%. The largest uncertainty is on the diameter because of limitations on machining.

4.2.2. Principle of calculation.

The propagation of stress waves along a cylindrical bar yields three types of vibrations:

1) The longitudinal waves propagate according to the wave equation: $\rho \frac{\partial^2 U}{\partial t^2} = E \frac{\partial^2 U}{\partial x^2}$ where U is the displacement along the direction x of propagation, E Young's modulus and ρ the density of the material. The waves propagate with a velocity $V_o = \sqrt{E/\rho}$, independent of their frequency, so long as the wavelength Λ is large with respect to the diameter d of the bar.

2) the torsional waves, which correspond to the rotations of plane sections, perpendicular to the axis, obey also the wave

equation: $\mu \frac{\partial^2 \theta}{\partial x^2} = \rho \frac{\partial^2 \theta}{\partial t^2}$ where θ is the angle of rotation of a plane section, and μ the second Lamé's coefficient. Their velocity is $\sqrt{\mu/\rho}$.

3) the flexural waves obey the equation: $\frac{\partial^2 W}{\partial t^2} = - C_o^2 K^2 \frac{\partial^4 W}{\partial x^4}$, where W is the displacement in the z-direction of flexion and K is the radius of gyration of the bar; here the group velocity for a pulse of energy to propagate is dependent on the wavelength: $C_g' = \frac{4\pi C_o K}{\Lambda}$.

Although exact solutions have not been obtained for a cylinder of finite length, solutions may be derived which give very good results so long as the ratio d/L is small. In Pochhammer's treatment[16], the general equations of motion of an isotropic elastic medium:

$$\rho \frac{\partial^2 U}{\partial t^2} = (\lambda+\mu) \frac{\partial \Delta}{\partial x} + \mu \nabla^2 U$$

$$\rho \frac{\partial^2 V}{\partial t^2} = (\lambda+\mu) \frac{\partial \Delta}{\partial y} + \mu \nabla^2 V$$

$$\rho \frac{\partial^2 W}{\partial t^2} = (\lambda+\mu) \frac{\partial \Delta}{\partial z} + \mu \nabla^2 W$$

are written into polar cylindrical coordinates r,θ,Z, with displacements u_r, u_θ, u_z:

$$\rho \frac{\partial^2 u_r}{\partial t^2} = (\lambda+\mu) \frac{\partial \Delta}{\partial r} - \frac{2\mu}{r} \frac{\partial \bar{\omega}_z}{\partial \theta} + 2\mu \frac{\partial \bar{\omega}_\theta}{\partial z}$$

$$\rho \frac{\partial^2 u_\theta}{\partial t^2} = (\lambda+\mu) \frac{1}{r} \frac{\partial \Delta}{\partial \theta} - 2\mu \frac{\partial \omega_r}{\partial z} + 2\mu \frac{\partial \omega_z}{\partial r}$$

$$\rho \frac{\partial^2 u_z}{\partial t^2} = (\lambda+\mu) \frac{\partial \Delta}{\partial t} - \frac{2\mu}{r} \frac{\partial}{\partial r}(r \omega_\theta) + \frac{2\mu}{r} \frac{\partial \omega_r}{\partial \theta}$$

where Δ is the dilatation, equal to:

$$\Delta = \frac{1}{r} \frac{\partial (r u_r)}{\partial r} + \frac{1}{r} \frac{\partial u_\theta}{\partial \theta} + \frac{\partial u_z}{\partial z}$$

and $\bar{\omega}_r, \bar{\omega}_\theta, \bar{\omega}_z$ are the components of the rotation about three orthogonal directions (along the radius-vector, perpendicular to the rz plane and parallel to the z-axis).

Pochhammer considers the propagation of an infinite train of sinusoidal waves along a solid cylinder and assumes displacements of the form:

$$\left| \begin{array}{l} u_r = U \exp i (\gamma z + p t) \\ u_\theta = V \exp i (\gamma z + p t) \\ u_z = W \exp i (\gamma z + p t) \end{array} \right.$$

where U,V,W are functions of r and θ only. The waves have a frequency $f = p/2\pi$ and a wavelength $\Lambda = 2\pi / \gamma$.

In the case of pure longitudinal waves, we assume that u_θ vanishes and that U and W are independent of θ. After some manipulation, U and W can be written as:

$$U = A \frac{\partial}{\partial r} J_o (h'r) + C \gamma J_1 (k'r)$$

$$W = A\, i \gamma J_o (h'r) + \frac{C\, i}{r} \frac{\partial}{\partial r} r J_1 (k'r)$$

where:

$$h'^2 = \frac{\rho p^2}{\lambda + 2\mu} - \gamma^2$$

$$k'^2 = \frac{\rho p^2}{\mu} - \gamma^2$$

A and C are constants and J_0 and J_1 Bessel's functions of order zero

and one.

Finally, the boundary condition of vanishing stress at r = a (where a = d/2 is the radius of the bar), gives the equations:

$$A\left[2\mu \left.\frac{\partial^2 J_o(h'r)}{\partial r^2}\right|_{r=a} - \frac{\lambda}{\lambda+2\mu} p^2 \rho\, J_o(h'a)\right] +$$

$$2\gamma C\mu \left.\frac{\partial J_1(k'r)}{\partial r}\right|_{r=a} = 0$$

$$2\, A\gamma \left.\frac{\partial J_o(h'r)}{\partial r}\right|_{r=a} + C\,(2\gamma^2 - \frac{p^2\rho}{\mu})\, J_1(k'a) = 0$$

On eliminating A and C, we obtain the so-called "frequency equation" in the following form (see Appendix for derivation):

$$(X - 1)^2\, \varphi(h'a) - (\beta X - 1)\left[X - \varphi(k'a)\right] = 0 \qquad (4.3)$$

where:

$$\varphi(y) = y\, \frac{J_o(y)}{J_1(y)}$$

$$X = (V/V_o)^2\, (1 + \sigma)$$

$$\beta = \frac{1 - 2\sigma}{1 - \sigma}$$

Note that the velocity of propagation V is equal to p/γ or $f\Lambda$. For σ given, this is an equation between V/V_o and a/Λ, which allows a determination of $E = \rho V_o^2$, or, E being known, to determine σ.

4.2.3. Outline of computation.

1) Computation of E.

For low modes of vibration (i.e., small a/Λ), the frequency equation is closely approximated by Rayleigh's equation:

$$\frac{V}{V_o} = 1 - \sigma^2 \pi^2 (a/\Lambda)^2 \qquad (4.4)$$

A good (or even approximate) guess of σ will yield an accurate value of E.

2) Computation of σ .

We should use the complete frequency equation; it is advisable, however, to transform it into a more practical form. First, the functions φ are closely approximated by continuous fractions:

$$\varphi = \mathcal{J}_1 = \frac{y\, J_o(y)}{J_1(y)} = 2 - \frac{y^2}{4} - \frac{y^2}{6} - \frac{y^2}{8} - \cdots$$

the four first terms being generally sufficient to determine φ accurately.[17] For computation purposes, it is easier, however, to define a new function $\theta(y) = y / \varphi(y)$. The frequency equation takes then the form:

$$F = (1 - X)^2 \, ih'a \, \theta(k'a) - (\beta X - 1) \, i\theta(h'a) \left[X \, \theta(k'a) - k'a \right] = 0 \qquad (4.5)$$

These computations were carried out on a LGP 30 electronic computer. The storage includes, besides useful numbers, the length, diameter, and mass of the specimen, the expansion coefficient, the measured frequencies of various modes for a number of significant temperatures. A special subroutine computes the function θ. The computer proceeds along the following steps:

2.1) Starting from L and d at room temperature, correct to L' and d' at temperature T.

2.2) Compute E from Rayleigh's equation. The first value of σ used is a guess; subsequently, the value of σ obtained from the previous temperature is used. Here, the values of the first mode only

are used:

$$\frac{V}{V_o} = \frac{f\Lambda}{\sqrt{E/\rho}} = 1 - \sigma^2 \pi^2 a^2 / \Lambda^2$$

2.3) Compute σ .

Starting from 0.28 as a first guess or the last computed value, compute X, β, γ , h'a and k'a, $\theta(h'a)$ and $\theta(k'a)$. The numerical value F of the left hand side of equation (4.5) is calculated and printed. In the range of values of interest for σ , F is a decreasing function of σ ; this is readily seen from the following numerical example with the curves given by Bancroft [18] guiding our choice of σ . When we choose the values $V/V_o = 0.9$, $a/\Lambda = 0.25$ and $\sigma = 0.50$, we get then: X = 1.215, β = 0, h'a = 1.571 i, k'a = 1.878. Since $\theta(y) = \frac{J_1(y)}{J_o(y)}$, the values of $\theta(k'a)$ and $\theta(h'a)$ are readily computed from Jahnke and Emde Tables. The value of F is then equal to -0.460. Therefore, if the guess on σ is too large, F is negative. The program was then set to change σ by increments of 0.005 until F changed sign, then of 0.001 until it changed again. The process is very rapidly converging; the convergence is checked, on the other hand, by printing all values of F for the various σ which are tried. The last value of σ is printed.

4.2.4. Estimate of accuracy.

As in resistance measurements, the uncertainty in temperature determinations is more related to a possible non equilibrium condition of the bath, than to the uncertainty in the reading itself. The determination of E from the first mode by Rayleigh's equation is accurate within 0.1%, the uncertainty coming mainly from the diameter and

Poisson's ratio values. So long as Pochhammer's treatment is justified, σ is calculated within 0.001, i.e., half of one percent.

4.3. HALL COEFFICIENT .

When a conductor is placed in a magnetic field perpendicular to the direction of current flow, a voltage is developed across the specimen in the direction perpendicular to both current and magnetic field; it is called the Hall voltage and, when a parallelepipedic specimen is used, is expressed by:

$$V_H = R_H \frac{B \times I}{t} \qquad (4.6)$$

where B is the magnetic induction, I the current intensity, t the thickness of the slab in the direction of the magnetic field.

This formula defines the Hall coefficient R_H expressed in practical units in volt. cm/amp. gauss. This quantity is particularly useful to provide information about the sign and concentration of charge carriers in the simplest cases. For identical carriers, a free electron model gives for the Hall coefficient: $R_H = \frac{1}{Nec}$ where N is the carrier concentration, e the electronic charge, c the velocity of light. The expression becomes quite complicated when two types of carriers contribute to the conductivity.

Another effect of interest is the change of resistance of the conductor, due to the magnetic field. A coefficient of magnetoresistance B_t is defined by: $\frac{\Delta R}{R_o} = B_t H^2$ for isothermal specimens in moderate fields; R_o is the initial resistance, ΔR the change in resistance due to the applied field, and H the field strength. An approximate theoretical expression for B_t has been derived by Mott and Jones[19].

4.3.1. Experimental methods.

The circuit and experimental arrangement used in these experiments are shown in Fig. 4 and 5.

The specimen carries a stable DC current and the DC voltage developed by the shift in equipotential lines due to the magnetic field is fed into a DC amplifier, then measured by a potentiometer. Similarly, the change in resistance in a magnetic field, can be observed as a change in voltage drop across the specimen between two resistance probes and measured by a potentiometer after DC amplification.

The circuitry used in this experiment is represented in Fig. 4; it is quite similar to the one used for resistance studies. The current and potential terminals are the same; in principle, one needs only to add two potential probes across the specimen in the "third"direction. Owing to the small magnitude of the effect, the presence of parasitic voltages, and the dependence of these voltage on some or all experimental variables (current I, magnetic field H, temperature T, contact potentials), special care must be taken in mounting the probes.

The voltage V_{AB} observed between the Hall potential probes A,B, is directly dependent through some functional relationship V(I,H,T) upon the three experimental factors we can control; let us call V_o = V(I,O,T), the voltage observed with zero magnetic field, when current intensity and temperature are stabilized. This voltage V_o is mainly due to:

1) A parasitic thermal emf V_{th}: any thermal gradient along

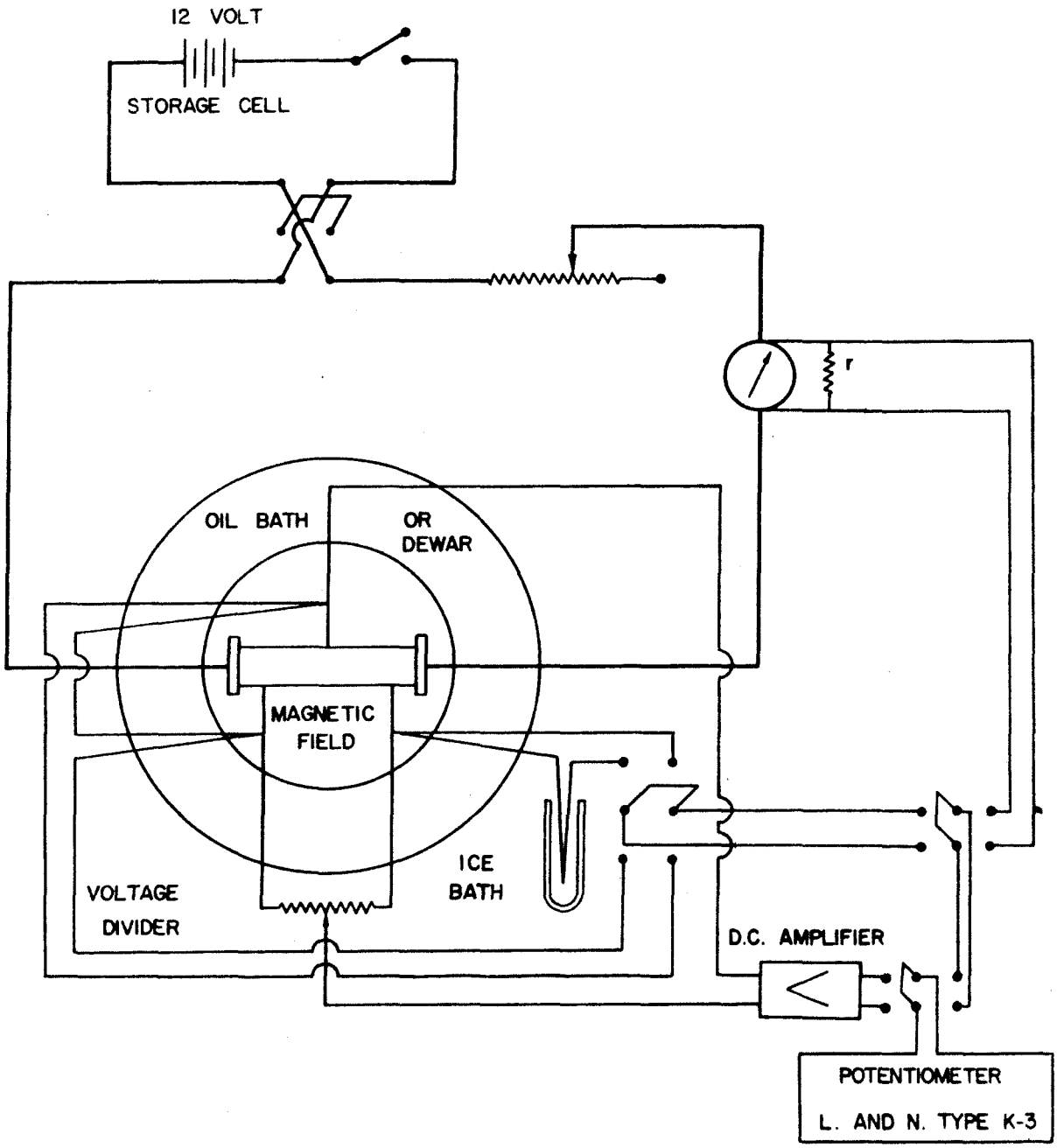

Fig. 4. Schematic diagram of the Hall effect circuit.

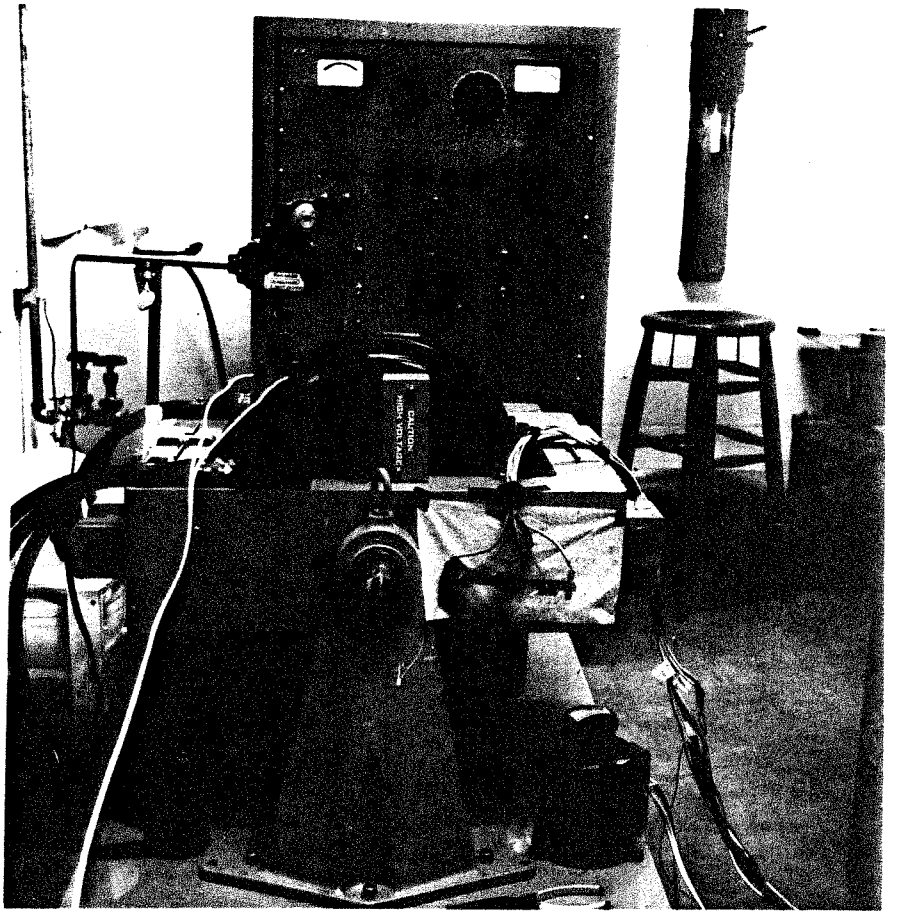

Fig. 5. General view of the magnetic measurements assembly. In the foreground, a specimen of chromium is shown, mounted for Hall effect and magnetoresistance measurements.

the specimen in the AB direction makes the two probes act as a thermocouple and yield an emf; its sign is independent of the signs of I and H, its magnitude is dependent mainly on the temperature difference between A and B.

2) An emf V_1 due to the misalignment of the probes with respect to the equipotential lines. The complexity of boundary conditions and the difficulty of the experimental setup make impossible a perfect alignment of the Hall probes on the same equipotential line in the specimen. Since the current must be turned on for some time before the experiment for temperature stabilization purposes, we observe an emf due to this misalignment; its sign is of course reversed by a reversal of the current.

Several experimental improvements are used to correct these parasitic emfs. As far as the thermal emf is concerned, the use of a constant temperature bath tends to improve temperature uniformity; it does not prevent, however, local thermal fluctuations, which become more important at higher temperatures. The emf due to the misalignment of the probes can be reduced to a negligible value by the following scheme: on one side of the specimen, two probes, about 3/8 in. apart, are connected to a 2 ohm voltage divider with a fine adjustment; the value of V_o can thus be brought down as close to zero (or to any convenient value) as the fineness of the divider can permit. The DC current through the specimen is obtained by connecting it in series with a 12 volt battery and a rheostat. A switch is provided to open the circuit and to reverse the direction of the current. An ammeter gives a coarse reading of the intensity; in order to get an accurate

measurement, the voltage drop across a 1 ohm resistor mounted in parallel with the ammeter, is measured by a potentiometer.

The magnetic field used in this study is obtained from a Varian Model V-4007 Six-inch Electromagnet, using 4 in. pole pieces with an air gap of 7/8 in. These conditions provide a maximum field of about 15.8 kilogauss, uniform within 1% over about 2 1/2 in. or within 10% over 3 1/2 in. The maximum length of the specimens investigated is within the 3 1/2 in. area. The magnetic field can be reversed through an automatic field-reversing mechanism provided in the power supply.

The bias voltage V_o with the superimposed Hall voltage $\pm V_H$ is fed into a low level DC voltage amplifier Leeds and Northrup 9835A; its output is fed into the Leeds and Northrup Type K-3 Universal Potentiometer. It is possible also to reverse the polarity of the potentiometer with respect to the emf and the galvanometer circuit.

Constant temperature conditions are obtained in the same way as for resistance studies above room temperature (only this range of temperatures was investigated in this study), as described in Part 4.1.2. The only extra precaution in these experiments is to turn on the magnet power supply and the coil water cooling system for a sufficient period of time to allow the bath to take equilibrium conditions with respect to its surroundings. Finally a thorough electrical shielding is provided, and the wires are rigidly mounted to minimize induced voltages in the measuring circuit.

4.3.2. Operating Procedure .

Sufficient time is first given for the oil bath temperature and for the battery current to reach equilibrium conditions; both the

bath temperature and the battery current are measured on the L&N K-3 Potentiometer. Under no magnetic field, the voltage $V_0 = V_{th} + V_1$ is measured, then $V_0' = V_{th} - V_1$, after reversal of the electric current in the specimen; these measurements are repeated several times and the value of $V_0 - V_0' = 2\ V_1$ is averaged in order to minimize the time variation of V_{th} between measurements. The magnetic field is then turned on, the voltages $V = V_{th} + (V_H + V_1)$ and $V' = V_{th} - (V_1 + V_H)$ are measured several times and their difference is averaged to yield $2\ V_1 + 2V_H$ and therefore V_H. Temperature and current intensity are read again, to check for any drift during the course of the experiment. The magnet current can be changed to get different fields; in this case, care is taken to change the current always in one direction, say, increasing fields.

4.3.3. Calculation of the Hall Coefficient.

From formula (4.6), we derive the value of the Hall coefficient at a given temperature: $R_H(T) = \frac{V_H \cdot t}{B.I}$. In view of the small absolute value of the paramagnetic susceptibility of chromium, the permeability is very close to one and the magnetic induction B will be taken equal to the magnetic field intensity H. As was explained previously, in 4.3.1., the current intensity I is measured from the voltage drop across a 1 Ω resistor mounted in parallel with the ammeter. The resistor has a high resistance (1.087 Ω) with respect to the ammeter (2.709 m Ω); we call v the voltage drop, I_A and I_R the intensities through the ammeter and the resistor respectively:

$$I = I_R + I_A$$

$$2.71\ I_A = 10^3 \times 1.087\ I_R = v\ (\text{m V})$$

hence I (amp) = 0.370 v (mV).

The magnetic field intensity, measured with a GRH Hennig Gaussmeter, is 15.8 $\pm$ 0.2 kilogauss at maximum magnet current (1.4 amp/section) and 7/8 in. air gap. In all measurements, only the highest field intensity is used.

The estimate of the thickness of the sample presents the same difficulty as for the resistance experiments. For the specimen BT, a number of measurements of the thickness gives an average of 0.0625 $\pm$ 0.0020 in. i.e., 0.0158 $\pm$ 0.0010 cm; for the specimen W1, the diameter is 0.628 $\pm$ 0.003 cm.

We derive the practical formulae for the two samples we used in maximum magnetic field, for a voltage amplification of 200:

1) Case of a strip (specimen BT)

$$R_H \left(\frac{\text{volt.cm}}{\text{amp.gauss}}\right) = \frac{V(\text{volt})\ t\ (\text{cm})}{H\ (\text{gauss})\ I\ (\text{amp})} = \frac{V_H\ (\mu V) \times 10^{-6} \times 0.158}{15800 \times v\ (\text{mV}) \times 0.37 \times 200}$$

$$\text{or} \quad R_H = \frac{V_H\ (\mu V)}{v\ (\text{mV})} \times 1.34 \times 10^{-13} \qquad (4.7)$$

2) Case of a rod (specimen W1)

In this case, we should use a more general relationship for the Hall voltage: $E_H = R_H\ H \times J$ where E_H is the "Hall field" and J the current density; therefore, with a rod of diameter d:

$$E_H = \frac{V_H}{d} = R_H \frac{H \times I}{\frac{\pi d}{4}^2}$$

or

$$V_H = R_H \frac{H.I}{\pi d/4} \quad ; \text{ the rod is equivalent to a strip}$$

with an "equivalent thickness" $t' = \pi d/4 = 0.628 \times \frac{\pi}{4} = 0.499$ in the

present case:

$$R_H \left(\frac{\text{volt. cm}}{\text{amp. gauss}}\right) = \frac{V_H \ (\mu V)}{v \ (mV)} \times 4.25 \times 10^{-13} \qquad (4.8)$$

4.3.4. Accuracy and limitations of the method.

There are two different categories of uncertainties involved in the method. First is the uncertainty related to the systematic errors in the determinations of H, t, and the angle between H and I. These uncertainties are respectively of the order of 1%, 2.5% and 0.5%; they are "systematic" in the sense that they are the same for all experimental determinations and yield a 4% uncertainty on the numerical factor of formulae (4.7) or (4.8). On the other hand, the determination of V_H and V involve experimental relative uncertainties; both voltages can be read within 0.5 μV on the K-3 potentiometer; the battery drift during one experiment produces a variation in V of a few microvolts at most, i.e., an uncertainty of 0.5%; in the observation of V_H, a "thermal" noise was detected, due to the lack of uniformity of the temperature of the bath, i.e., rapid variations of temperature in the vicinity of the probes, with a "period" of the order of magnitude of or smaller than the time required to complete a measurement; this noise becomes increasingly troublesome as the temperature of the bath is raised, requiring more measurements to be taken and averaged, and the time between measurements with reversal of current to be kept as short as possible; this difficulty is the major drawback of the method, increasing the uncertainty of measurements from about 1% at room temperature to about 5% at 100 C, and giving larger spread in the experimental points.

4.4. PRINCIPLE OF MAGNETORESISTANCE MEASUREMENTS.

In order to measure the relative change in resistance $\frac{\Delta X}{X}$ due to an applied magnetic field, the resistance under study X is placed in an ordinary Kelvin Bridge; the bridge is balanced, first under zero magnetic field; then, when the field is applied, the small unbalanced voltage appearing in the diagonal, as a result of the change of resistance ΔX, is amplified and measured on the potentiometer.

With the symbols used in Fig. 6, the voltage U across the diagonal of the bridge is: $U = (X + \rho_1)\, i_1 - A\, i_2$

or, since $i_1 = \dfrac{I\,(A + B)}{X + \rho_1 + \rho_2 + R + A + B}$ and

$$i_2 = \frac{I(X + \rho_1 + \rho_2 + R)}{X + \rho_1 + \rho_2 + R + A + B} \quad ,$$

$$U = I \; \frac{(X + \rho_1)\, B - A\,(R + \rho_2)}{X + \rho_1 + \rho_2 + R + A + B} \; .$$

Therefore

$$\delta U = I \; \frac{(A + B)\,(B + R + \rho_2)}{(X + \rho_1 + \rho_2 + R + A + B)^2} \quad \Delta X .$$

Now, the usual Kelvin bridge set up is such that A and B are much larger than all other resistances; therefore:

$$\delta U \sim I \; \frac{(A+B)\,B}{(A+B)^2} \quad \Delta X \sim I \; \frac{\Delta X}{1 + \frac{A}{B}}$$

Usually the ratio A/B is, for instance 100/1000 = 0.1; then δU is of the order of $I\,\Delta X$.

It is difficult to estimate the magnitude of the effect to be expected; from the data published by Kapitza[20] on the magnetoresistance of chromium, the quantity $\frac{\Delta X}{X}$ seems negligibly small at room

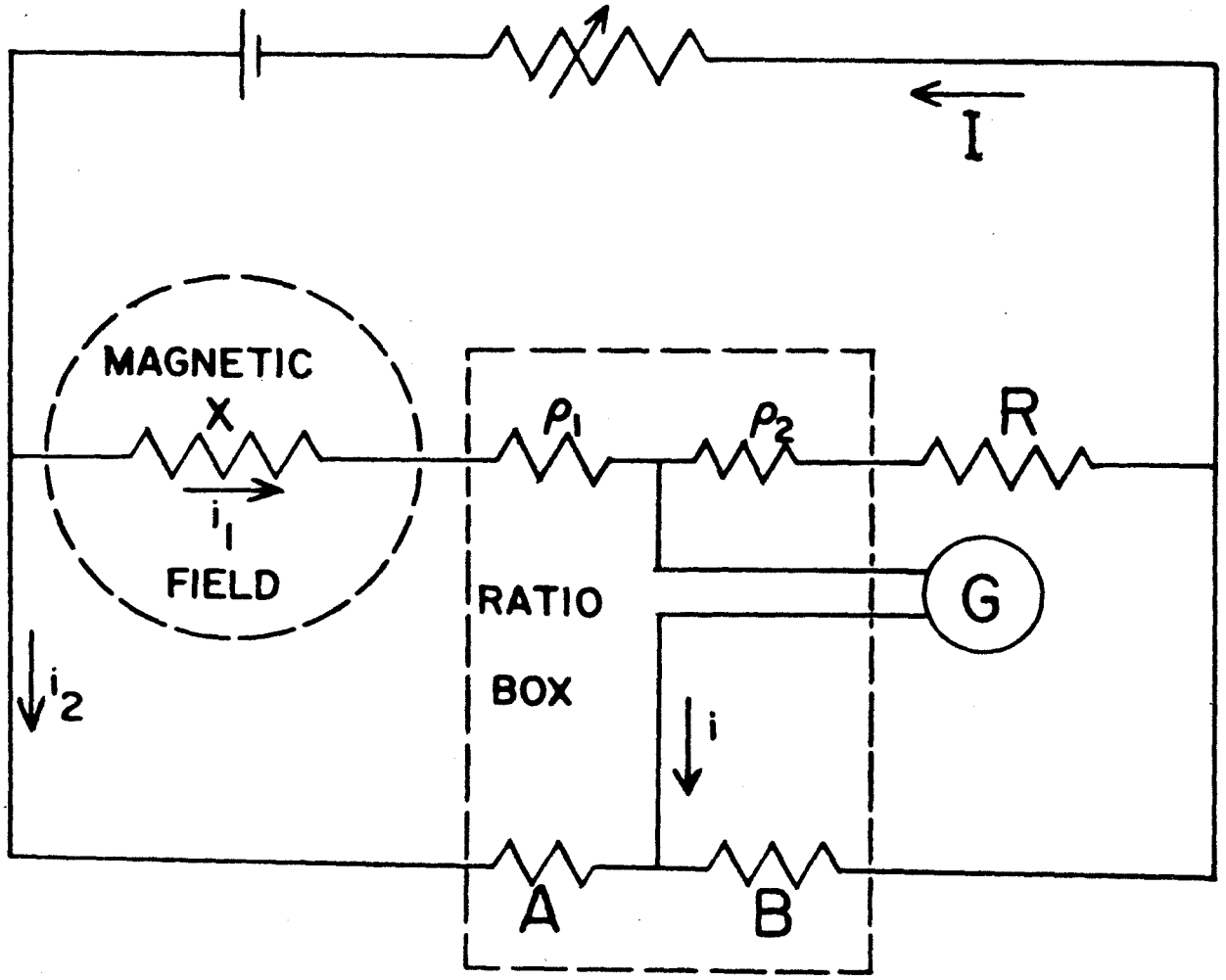

Fig. 6. Reduced diagram of magnetoresistance circuit.

temperature and in moderate fields up to 100 kilogauss; moreover, the coefficient B_t appears to increase strongly with increasing magnetic fields. It seems reasonable, however, to assume that the coefficient B_t in chromium is of the order of $10^{-12}(\text{gauss})^{-2}$, which is also of the order of magnitude of B_t in titanium[21]. With the field and resistance we use in these experiments, we can expect therefore a ΔX of $0.1\mu\Omega$ i.e. a voltage change δU after amplification of a few μV.

Although a voltage of this magnitude could be detected in principle, the larger distance between the probes on the specimen increases the effect of the local temperature fluctuations which were already mentioned for Hall effect measurements, and the method failed to detect any magnetoresistive effect. These thermal fluctuations leave little hope for the use of a DC method of this type for magnetoresistance determinations, at least with the low resistance specimens and relatively weak fields which have been used.

4.5. SPECIFIC HEAT.

4.5.1. Principle of the method of thermal analysis.

A method has been devised to measure the energy content of chromium specimens in a temperature range including the transition temperature. As this quantity was expected to be small, a method of differential thermal analysis was used: two geometrically similar specimens, one made of chromium and the other made of copper, are simultaneously heated and cooled in vacuo and their instantaneous temperature difference is continuously amplified and recorded.

The advantages of this method over the more usual methods of specific heat determinations are threefold: 1) A slow, controlled

rate of heating and cooling allows an instantaneous knowledge of the thermal properties of the specimen at a given temperature (other specific heat measuring techniques give rather total integrated results, over a range of temperatures). 2) Measuring a difference of temperature between two similar specimens with like thermal properties allows a high sensitivity in disclosing small variations. 3) Any accidental perturbation will affect both specimens in a similar way, but will have a small effect on the difference between the temperature of the two specimens.

The method, however, has the disadvantage of providing rather complicated relationships between experimental data and specific heat.

4.5.2. Operating procedure.

Two specimens, one of copper and one of chromium (sample WR) in the shape of small cylindrical rods are machined to the same external dimensions (length 4.2. cm, diameter 0.92 cm) to provide similar geometrical conditions for heat losses. Both specimens have a cylindrical hole along their axis (0.22 cm diameter for the Cu sample, 0.16 cm for the Cr sample), these last dimensions being adjusted to make the heat capacities of the two specimens approximately equal at room temperature.

Around each specimen, a given length of heating wire is wound (34 turns per specimen) and these two coils are connected in series. The heating wire consists of a Kanthal wire embedded in a dense magnesia insulation, with an outer stainless steel sheath of 0.7 mm diameter. The extremities of the heating wire are connected in series with a 12 V battery and a rheostat, to allow different heating rates.

Two Copper-Constantan thermocouples facing each other are located in the central part of the hole of each specimen (Fig. 7). These thermocouples measure: 1) the instantaneous temperature difference ΔT between the two specimens; 2) the temperature T of the Cr sample; 3) the temperature difference δT between the Cu sample and the surroundings. The temperature difference ΔT is amplified 200 times through a DC voltage amplifier and a ΔT versus T curve is continuously recorded (Fig. 8). The thermocouple junctions are soldered to small copper cylinders fitting tightly in the sample, to provide a good thermal contact with the specimens.

The samples and attached wires are placed in a 3 feet high Dewar, the inside of which can be evacuated; in this experiment, the pressure is kept constant at about 200 μ Hg. The thermocouple and heating wires are brought outside through a glass-to-metal seal, attached to a bakelite cap which rests through an O-ring on the flat circular edge of the Dewar, pressed down by atmospheric pressure.

In experiments below room temperature, measurements can be made only while the samples are heated from liquid nitrogen temperature to room temperature; in experiments above room temperature, measurements can be made while the samples are being either heated or cooled.

4.5.3. Derivation of formulae for specific heat calculations.

We derive below the formulae giving the temperature difference between two samples when they are heated or cooled simultaneously; the ambiant temperature will be referred to as T_o, T is the temperature of the sample after a time t, the initial temperature of the sample being T', and its mass m. The symbols with a subscript 1 refer to the

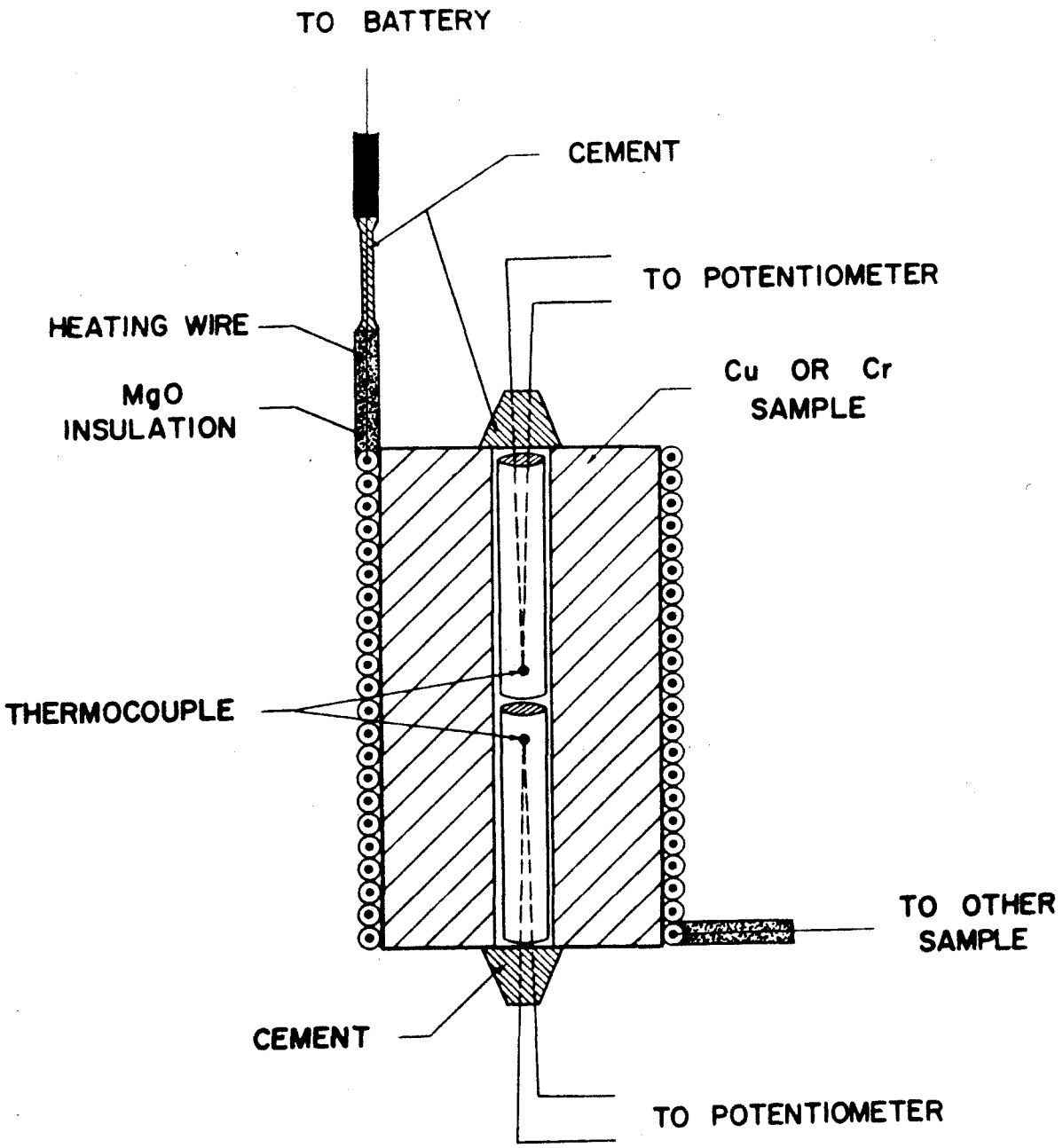

Fig. 7. Sketch of the mounting of a specimen in specific heat experiments.

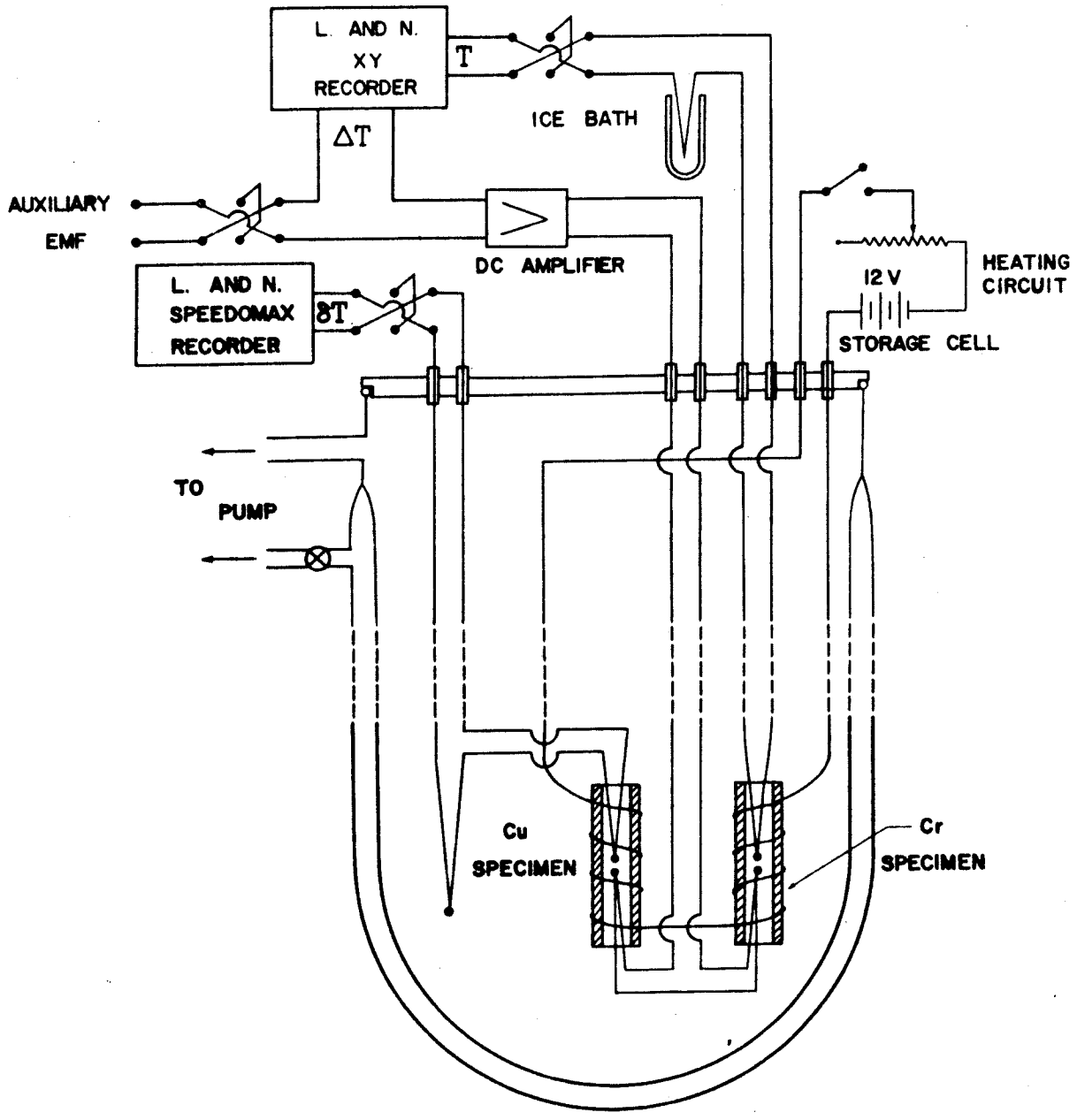

Fig. 8. Schematic diagram of the experimental assembly and recording circuit in specific heat determination.

chromium sample and those with a subscript 2 to the Copper sample.

4.5.3.1. Comparison of the magnitudes of radiation and convection processes.

The heat transfer from the specimen to the surroundings takes place by radiation and convection. Each specimen is essentially a cylinder of diameter d = 1 cm and height h = 2.4 cm; the two specimens are completely enclosed in a large reflecting enclosure of 20 cm diameter. The air is at constant temperature (22 C) and constant pressure (200 μ Hg); the temperature of the specimen varies from 22C to 70C, the temperature of interest being around 36C.

In the radiation process[22] the net heat exchange between a specimen and its surroundings is given by:

$$q = \sigma F_e F_a A_1 (T_1^4 - T_0^4) \qquad (4.9)$$

where σ is Stefan-Boltzmann's constant. Since the size of the cylindrical specimen is small with respect to the size of the enclosing cavity, the emissivity factor F_e is approximately equal to the emissivity of the surface of the specimen, i.e., of the outside tubing of the heater, estimated to be 0.5. The configuration factor F_a is taken equal to 1, for the same reason. The radiating area A_1 is equal to: $\frac{\pi d^2}{4} \frac{\pi}{2} + 2 \frac{\pi d^2}{4} = 6.6 \text{ cm}^2$. The temperature of the emitting specimen is taken as the temperature of the observed anomaly, 309 K, and room temperature as 295 K.

Inserting these values into Equation (4.9) and taking $\sigma = 0.57 \times 10^{-4}$ in cgs units we find:

$$q(\text{erg per second}) = \sigma F_e F_a A_1 T_0^4 \left[(T_1 / T_0)^4 - 1 \right]$$

$= 0.57 \times 10^{-4} \times 0.5 \times 6.6 \times 76 \times 10^{8} \ (1.20 - 1)$

$= 29 \times 10^{4}$ erg per second.

In the convection process[22], a coefficient of convection h_c is usually defined as $h_c = \frac{q}{T_1 - T_0}$. The coefficient h_c can be expressed as $(a\, L^3\, \Delta t)$ where a is a modulus for air (equal to 1.2×10^{6} (cu. ft.)$^{-1}$ at atmospheric pressure and 100F), L is the "equivalent length", defined by $\frac{1}{L} = \frac{1}{d} + \frac{1}{h}$ in the case of small vertical cylinders (here L = 8 cm = 27×10^{-3} ft) and Δt is the mean temperature difference between the specimen and the surroundings (taken here as 25F). Therefore $(a\, L^3\, \Delta t) = 1.2 \times 10^{6} \times 20 \times 10^{-6} \times 25 = 600$ at atmospheric pressure, and, in this case, $h_c = C \frac{K}{L} (a\, L^3\, \Delta t)^{1/4}$, where K is the thermal conductivity of air, equal to 0.016 B.t.u. per hour . foot . deg F and C is a constant approximately equal to 0.5. Then $h_c = \frac{0.5 \times 0.016}{27 \times 10^{-3}} (600)^{1/4} = 1.47$; now, h_c is dependent on air pressure through the modulus a, which is proportional to the square of the pressure expressed in atmospheres; in our experiment, $p = 200 \mu$Hg $= 2.7 \times 10^{-4}$ atm., hence $h_c = 2.4 \times 10^{-2}$. The heat exchange q is then equal to:

$q = h_c (T_1 - T_0) = 2.4 \times 10^{-2} \times 25$ B.t.u. per hour . square foot

$= \frac{2.4 \times 10^{-2} \times 25}{3.6 \times 10^{3}} \times \frac{6.6}{(12 \times 2.5)^2} \times 1055 \times 10^{7}$ erg per second

$= 1.3 \times 10^{4}$ erg per second.

These results indicate that the predominant mechanism of heat transfer in the present experiment is that of radiation, and consequently, the heat transferred by convection will be neglected in the

following computations.

4.5.3.2. Relationships between specific heat and temperature of the specimens.

Let us consider first a sample being cooled from T_1' to T_0. During the time dt, the sample cools from T_1 to $T_1 - dT_1$, involving a quantity of heat dq_1 such that: $dq_1 = -m_1 C_1 dT_1 - f_1 (T_1^4 - T_0^4) dt$ where $f_1 = \sigma F_e F_a A_1$ or:

$$dt = \frac{-m_1 C_1}{f_1 T_0^3} \quad \frac{d(T_1/T_0)}{(T_1/T_0)^4 - 1} \quad . \quad \text{Defining: } \alpha = \frac{f_1 T_0^3}{m_1 C_1}$$

and $x = \frac{T_1}{T_0}$, we can write:

$$\alpha \, dt = \frac{-dx}{x^4 - 1} \tag{4.10}$$

We call x_0 the temperature ratio $\frac{T_1'}{T_0}$, corresponding to the initial temperature. When integrated, Equation (4.10) reads:

$$\alpha \int_0^t dt = \alpha t = \int_{x_0}^{x} \frac{-dx}{x^4 - 1} = \frac{1}{2} \tan^{-1} x \Big|_{x_0}^{x} + \frac{1}{4} \ln \frac{(x+1)}{(x-1)} \Big|_{x_0}^{x} .$$

In the case of a sample heated from T_0 to T_1' at a rate r, and using the same notation, we find: $dq_1 = r\,dt = m_1 C_1 dT_1 + f_1 (T_1^4 - T_0^4) dt$ or:

$$dt = \frac{dx}{\frac{T_0^3 f_1}{m_1 C_1} \left[\left(1 + \frac{r}{f_1 T_0^4}\right) - x^4 \right]} \tag{4.11}$$

Defining now: $a^4 = 1 + \frac{r}{f_1 T_0^4}$ with $a > 0$, and $\beta = \frac{T_0^3 f_1}{m_1 C_1}$, equation (4.11) reads upon integration:

$$\beta \int_0^t dt = \beta\, t = \int_1^x \frac{dx}{a^4 - x^4} = \frac{1}{2\,a^3} \tan^{-1} \frac{x}{a} \Bigg|_1^x$$

$$+ \frac{1}{4\,a^3} \ln \frac{(x+a)}{(x-a)} \Bigg|_1^x$$

Finally, in the case of two samples being heated or cooled simultaneously, we can assume that the quantities r, f, T_0, are the same for both samples, since they have the same geometrical factors, as was explained in 4.5.2. Therefore, the coefficients a_1 and a_2 are equal, but $\alpha_1 \neq \alpha_2$ and $\beta_1 \neq \beta_2$ since they depend on C_1 and C_2.

The ratio of the heat capacities of the two samples at a given time is therefore given by:

$$\alpha_2/\alpha_1 = \frac{m_1 C_1 \tan^{-1} x_2 - \tan^{-1} x_0 + \frac{1}{2} \ln \left[(x_2 + 1)(x_0 - 1)/(x_2 - 1)(x_0 + 1)\right]}{m_2 C_2 \tan^{-1} x_1 - \tan^{-1} x_0 + \frac{1}{2} \ln \left[(x_1 + 1)(x_0 - 1)/(x_1 - 1)(x_0 + 1)\right]} \tag{4.12}$$

during a cooling experiment, and by:

$$\beta_2/\beta_1 = \frac{m_1 C_1 \tan^{-1}(x_2/a) - \tan^{-1}(1/a) + \frac{1}{2} \ln \left[(x_2 + a)(1 - a)/(x_2 - a)(1 + a)\right]}{m_2 C_2 \tan^{-1}(x_1/a) - \tan^{-1}(1/a) + \frac{1}{2} \ln \left[(x_1 + a)(1 - a)/(x_1 - a)(1 + a)\right]} \tag{4.13}$$

during a heating experiment.

4.5.4. Interpretation and accuracy of measurements.

It should be emphasized that the method just described is not well suited for accurate determinations of absolute values of specific heat. Only the ratio of the specific heat of chromium to that of copper is

determined at each temperature; at every instant, T_1 and ΔT (and therefore T_2, since $T_2 = T_1 - \Delta T$) are known from the recording; the coefficient a can be determined directly since by definition, $a \doteq \left(1 + \frac{r}{f_1 T_0^4}\right)^{1/4}$, but it is more accurate to obtain it from the equilibrium temperature at which the total heat input is compensated by radiation losses: under equilibrium conditions, $x_1 = x_1' = a$, hence $a = T_1/T_0$. Equations (4.12) and (4.13) show that the heat capacity of chromium is computed from: $m_1 C_1 = (\alpha_2/\alpha_1) m_2 C_2$ or $(\beta_2/\beta_1)\ m_2 C_2$. The ratios α_2/α_1 and β_2/β_1 are determined from these experiments, and $m_2 C_2$ has to be theoretically computed: $m_2 C_2 = m_2\ (C_V\ (1 + AT) + \gamma T)$. The specific heat C_v at constant volume is obtained from the universal curve $C_v = f\ (\theta / T)$ given by the Landolt-Bornstein Tables, by taking the Debye temperature of copper as 445 K. The coefficient A for conversion to specific heat at constant pressure, is equal [23] to 1.0×10^{-4} (deg K)$^{-1}$ and the term γ for the electronic contribution equal [24] to 1.79×10^{-4} cal per mole. (deg K)^2. The variation of $m_2 C_2$ with temperature is represented on Fig. 9.

The sensitivity of the temperature recording circuit is such that one inch on the horizontal scale of the chart corresponds to 0.13 degree C, i.e., a variation of a few hundredths of one degree in the temperature difference between the two specimens can be detected. In these experiments, the choice of the rate of heating is very important; if it is too high, in the sense that the specimens go too fast through the region of temperatures of interest, the phenomenon to be observed may well fail to be detected. In the experiments above

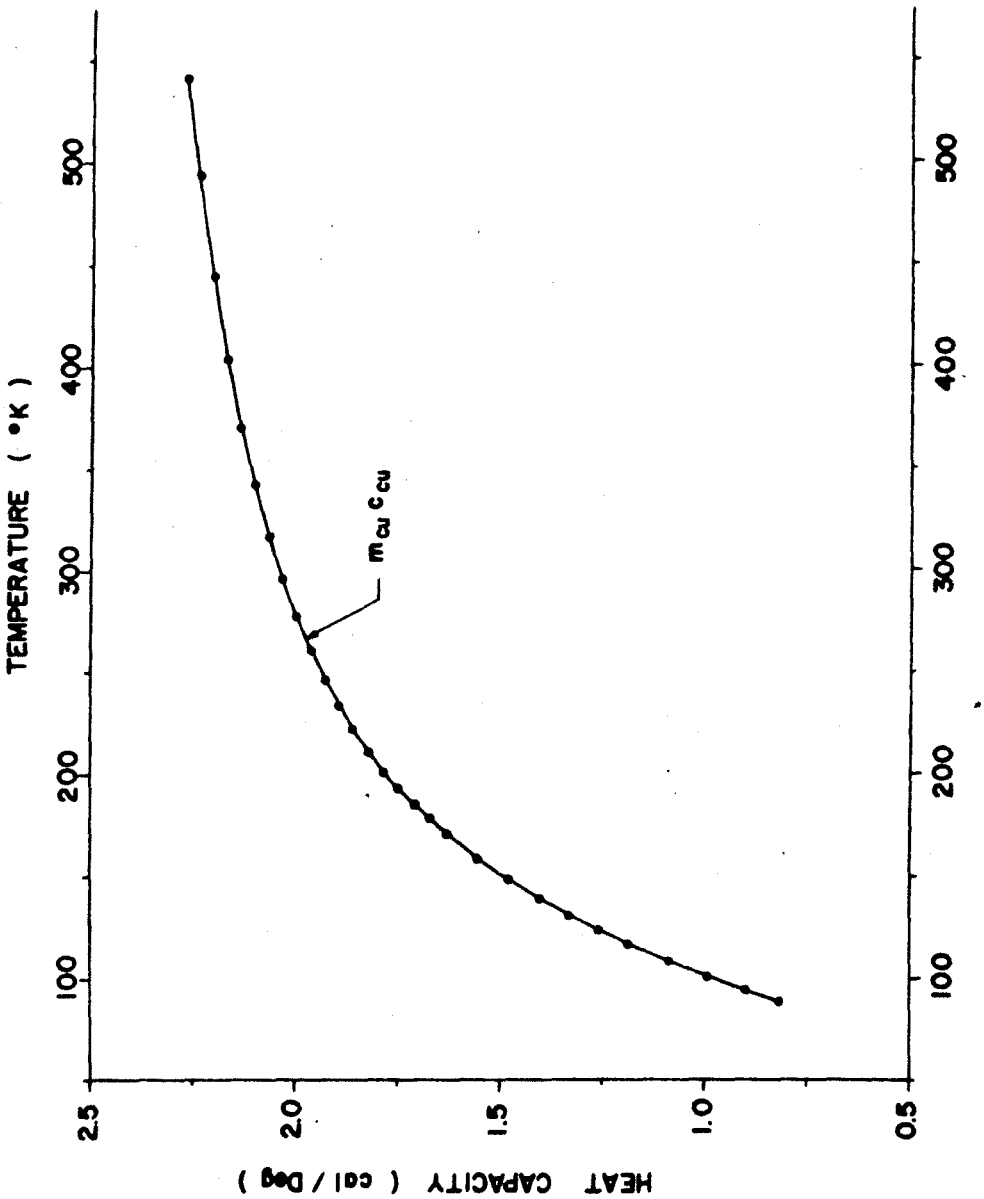

Fig. 9. Computed variation with temperature of the heat capacity of the copper specimen.

room temperature, the rate of heating could be kept as low as 5 C/ hour; in the experiments below room temperature, the rate of heating was of the order of 3 C/minute and therefore too fast to detect a small variation in specific heat over a narrow range of temperatures.

V. EXPERIMENTAL RESULTS

Around the transition temperatures in chromium, anomalies have been found in the measurements of electrical resistivity, Young's modulus and Poisson's ratio, Hall coefficient, specific heat; these physical properties are discussed below in four separate sections and a summary of the experimental results is presented in Table II.

5.1. ELECTRICAL RESISTIVITY .

The results of measurements of the electrical resistance of the five specimens investigated are plotted in Fig. 10 on an arbitrary scale. All these curves have some important features in common: the resistance increases roughly linearly, both in the low temperature region (from - 195C to about 0 C) and in the high temperature region (above 65 C), but with a much lower slope at high temperatures. These two regions are connected by a transition range, presented in Fig. 11 for the five specimens investigated. In this region, the temperature coefficient of resistance changes continuously; it is monotonic for one specimen only (BM2') and shows a marked minimum for all others: this minimum is close to zero for two specimens (WR and BT), slightly negative for BM3 and markedly negative for W1.

From the rather complex shape of the resistance curve in the critical region, it is somewhat difficult to define one transition temperature. By convention, such a temperature could be chosen at the inflexion point or at the minimum when they exist or, preferably, at the end of the transition range, i.e., the lowest temperature of

TABLE II

SPECIMEN	RESISTIVITY	YOUNG'S MODULUS & POISSON'S RATIO	HALL EFFECT	SPECIFIC HEAT
BM I - II	T_e = 65 C ρ_0 = 15.7$\mu\Omega$x cm R_0 = 218 $\mu\Omega$ a_{1-u} = 4.10 &1.38x10^{-3}(C)$^{-1}$	Low temperature trans. ΔE = 3% T_l=-149C $\Delta\sigma$ = 3% High temperature trans. T_u = 59C ΔE = 10% $\Delta\sigma$ = very large		
BM III	T_i = 36 C, T_e = 42 C ρ_0 = 13.6$\mu\Omega$x cm R_0 = 2046 $\mu\Omega$ a_{1-u} = 3.58&3.03 x 10^{-3}(C)$^{-1}$			
W 1	T_i = 25 C, T_e = 33 C ρ_0 = 14.8$\mu\Omega$x cm R_0 = 221 $\mu\Omega$ a_{1-u}=3.77&2.60x10^{-3}(C)$^{-1}$	Low temperature trans. T_l = -168C ΔE = 0.5% $\Delta\sigma$ = 1% High temperature trans. T_u = 25 C ΔE = 2% $\Delta\sigma$ = 6%	R_H = 28x10^{-13} volt.cm / amp.gauss Break in slope at 35 C from - 0.45 to -0.05 volt.cm / amp.gauss(C)	
BT	T_i = 37 C, T_e = 44 C ρ_0 = 12.8$\mu\Omega$x cm R_0 = 493 $\mu\Omega$ a_{1-u}=3.96&2.86x10^{-3}(C)$^{-1}$		R_H=33x10^{-13} volt.cm / amp.gauss Break in slope at 42C from -0.45 to -0.05 volt.cm / amp.gauss(C)	
WR	T_i = 33 C, T_e = 42 C ρ_0 = 13.2$\mu\Omega$x cm R_0 = 188 $\mu\Omega$ a_{1-u}=4.35&2.81X10^{-3}(C)$^{-1}$			8% peak at 36 C

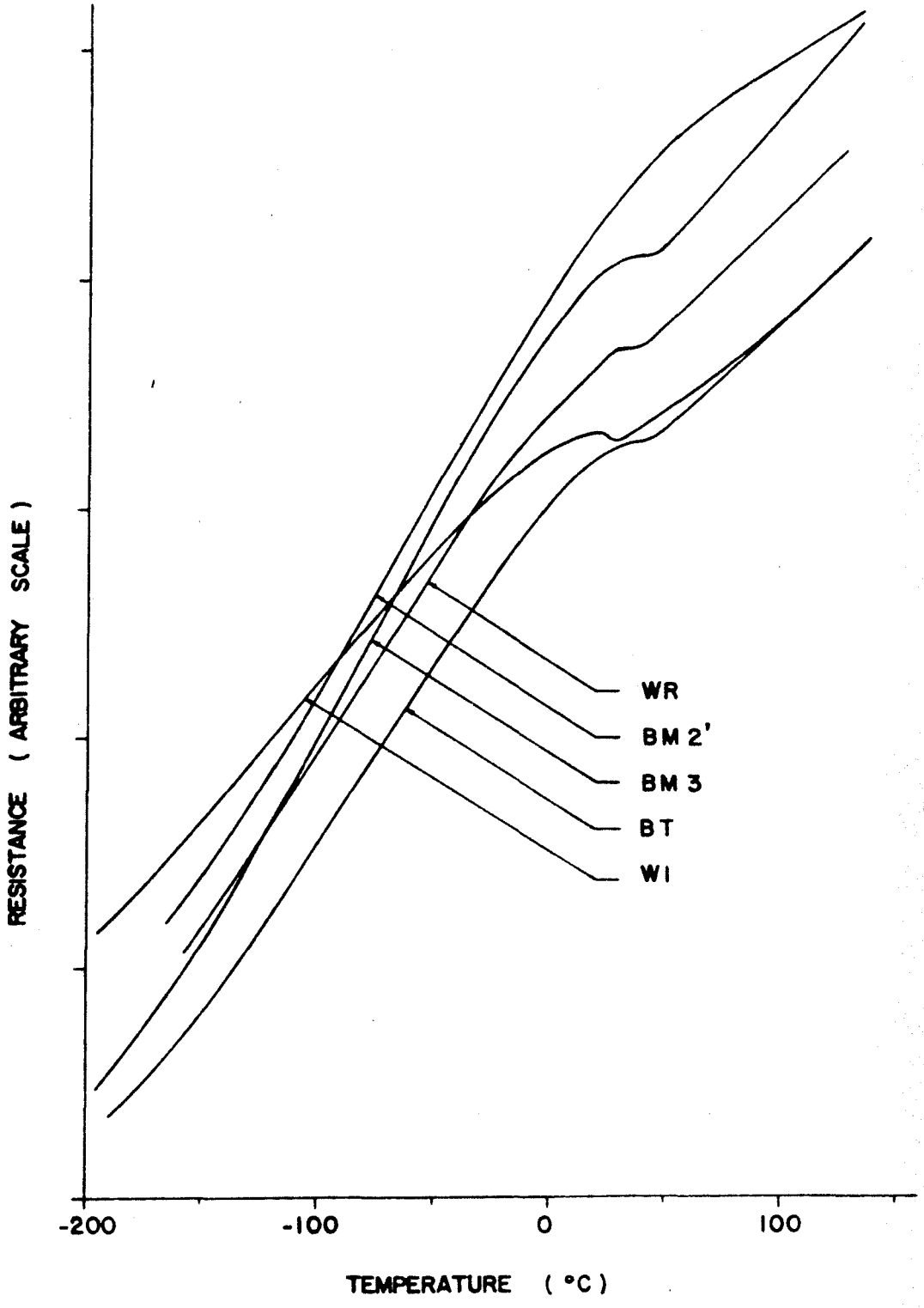

Fig. 10. Electrical resistance versus temperature curves for five chromium specimens.

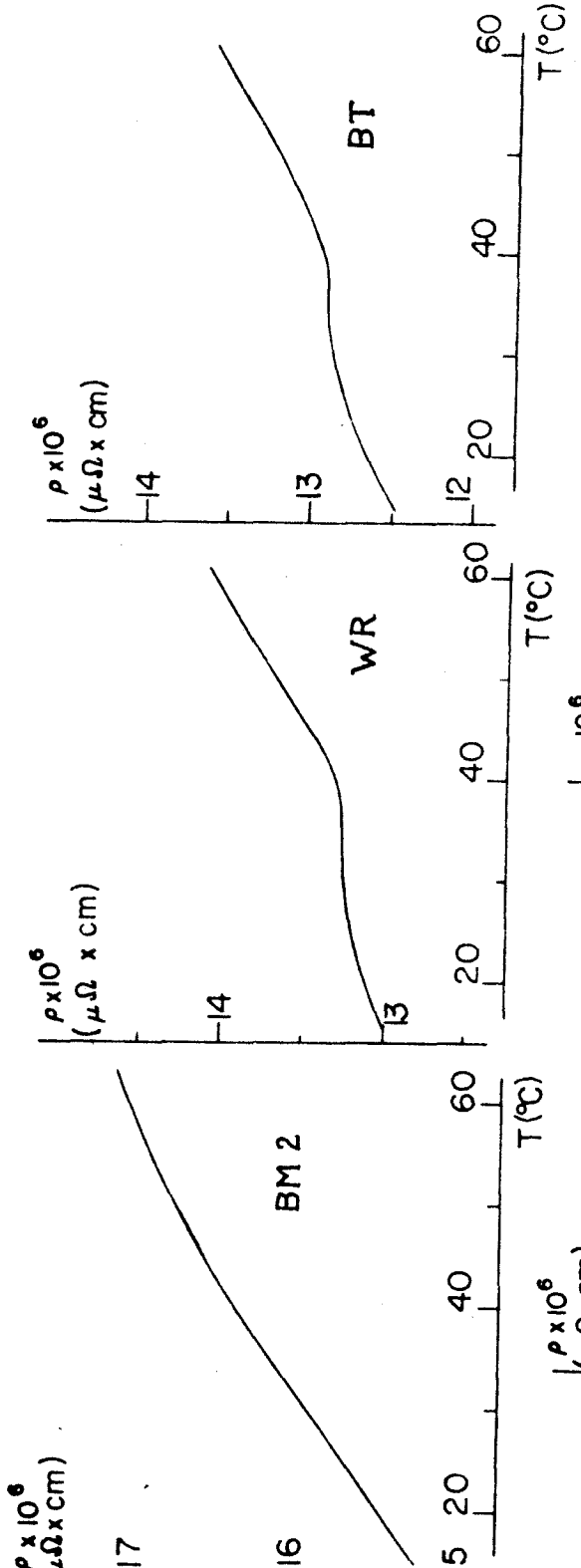

Fig. 11. Electrical resistivity versus temperature curves in the transition region.

the linear high temperature region. In most cases, temperatures corresponding to both the inflexion point T_i and to the end of the transition T_e are reported in Table II, together with the estimated resistivity ρ_o at 25 C, the resistance R_o at 25 C and $a = \frac{1}{R_o} \frac{dR}{dT}$ (respectively a_l for the lower region and a_u for the upper region of the linear variation).

The values of the resistivity at room temperature for the five specimens investigated are in fair agreement with one another and with other published data[2,8]. The mean value of the present results is 14.0 $\mu\Omega$. cm and the spread about this value, roughly $\pm$ 1.5 $\mu\Omega$. cm, is probably due to the presence of impurities and to the proximity of the transition temperature. Fig. 12 and 13 show the small apparent hysteresis between heating and cooling experiments, due to non-equilibrium temperature conditions in the bath.

The connection between resistivity and resistance should also be considered in view of the large anomaly in the expansion coefficient reported by Fine et al[8]. Resistance, indeed, depends both on the resistivity ρ and on the dimension factor $\frac{1}{S}$, since $R = \rho \left(\frac{1}{S}\right)$. Let us define the temperature coefficients: $r = \frac{1}{R} \frac{dR}{dT}$, $p = \frac{1}{\rho} \frac{d\rho}{dT}$, $\alpha = \frac{1}{l} \frac{dl}{dT}$, $\beta = \frac{1}{S} \frac{dS}{dT}$. Differentiating the formula $R = \rho \left(\frac{1}{S}\right)$ and assuming isotropic expansion, i.e., $\beta = 2\alpha$, we get: $p = r + \alpha$. From the results of Fine et al[8], the expansivity anomaly is a contraction corresponding to a minimum in α from about 6 to 1 x 10^{-6} $(C)^{-1}$; from the results of the present investigation, the resistance anomaly corresponds also to a decrease in the coefficient r in the transition region, of the order of 4 x 10^{-3} $(C)^{-1}$; both anomalies tend to make p

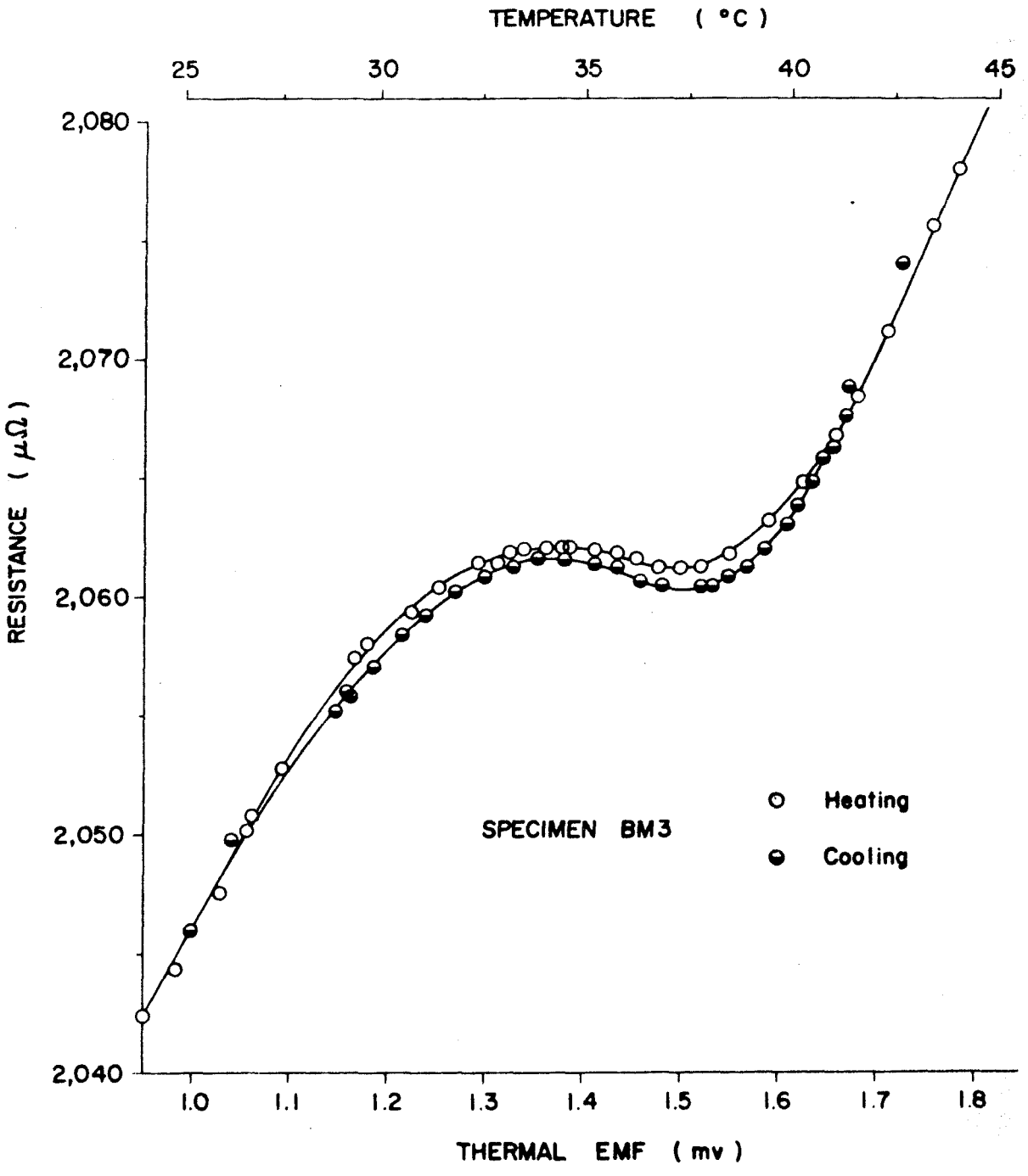

Fig. 12. Electrical resistance versus temperature curve in the transition region of specimen BM 3.

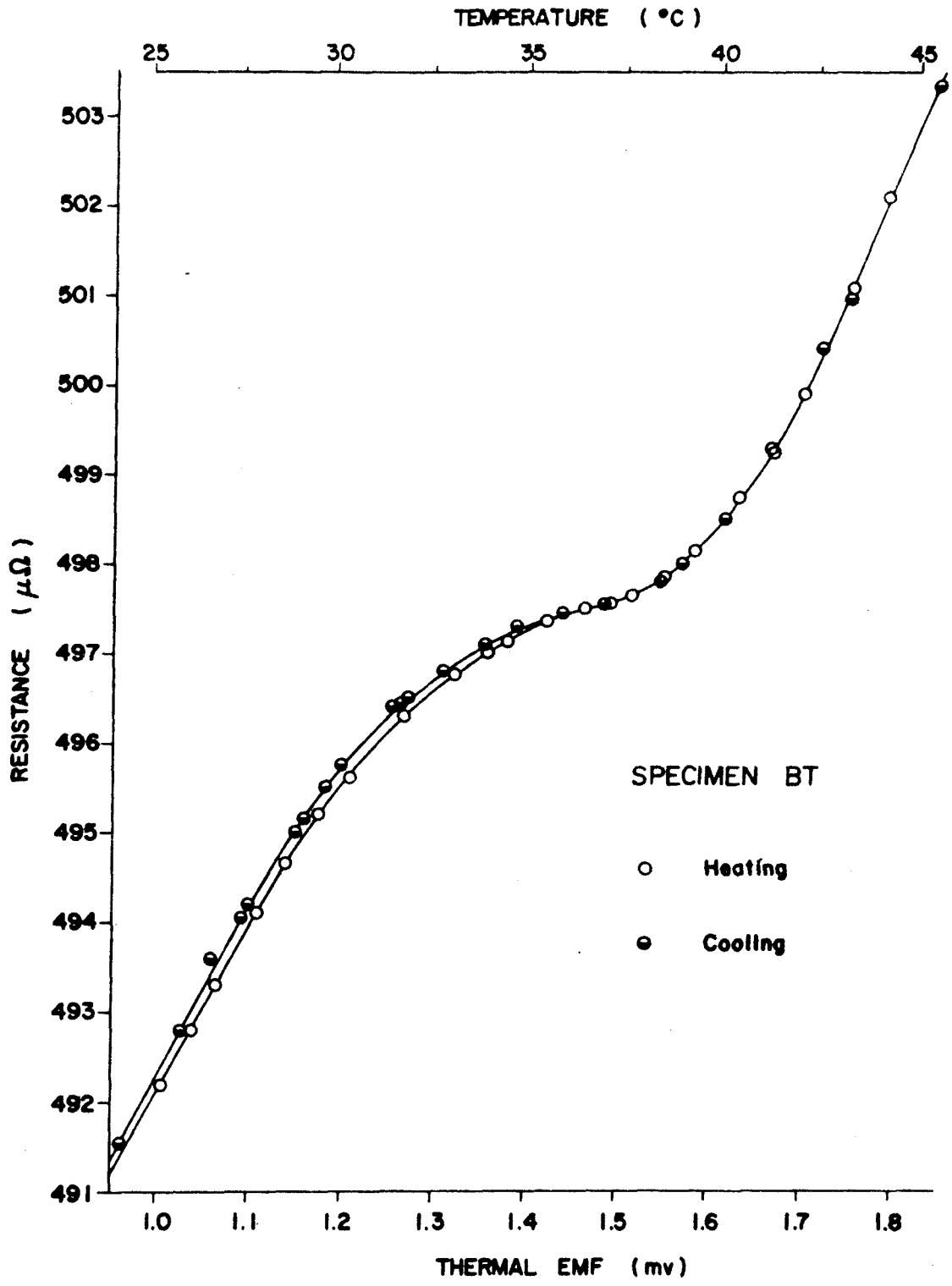

Fig. 13. Electrical resistance versus temperature curve in the transition region of specimen BT.

minimum at the transition, but the effect of the expansion anomaly is negligible. The anomaly in resistance therefore corresponds to an actual anomaly in resistivity of the same order of magnitude.

5.2. YOUNG'S MODULUS AND POISSON'S RATIO.

The experimental results for Young's modulus versus temperature are presented in Fig. 14 for specimens BM1 and W1, together with the results of Fine, Greiner, Ellis[8] (dotted curve, labeled FGE). Fig. 15 shows the variation with temperature of the frequency of the first mode of vibration for specimen BM2'. The main features of the observed anomalies are also summarized in Table II.

The actual shape of the anomalous region of the Young's modulus E versus temperature curve around the transition temperature differs widely from specimen to specimen; here, the transition temperature is arbitrarily defined as the temperature at which the E versus temperature curve has a minimum. When compared with the previously published results[8], the anomalies measured on specimens BM1 and BM2' have a larger amplitude, a wider temperature range and they occur at higher temperatures. On the other hand, the anomalies for specimen W1 have a smaller amplitude, and occur at a lower temperature.

The variation with temperature of Poisson's ratio for specimens BM2' and W1 is presented in Fig. 16. These curves display the same general shape of anomalies as the E versus temperature curves. For specimen BM2', Poisson's ratio could not be reliably computed near the transition temperature, because of the very rapid variation of Young's modulus (see 4.2.3.).

The variation of the frequency of the first mode in the transition

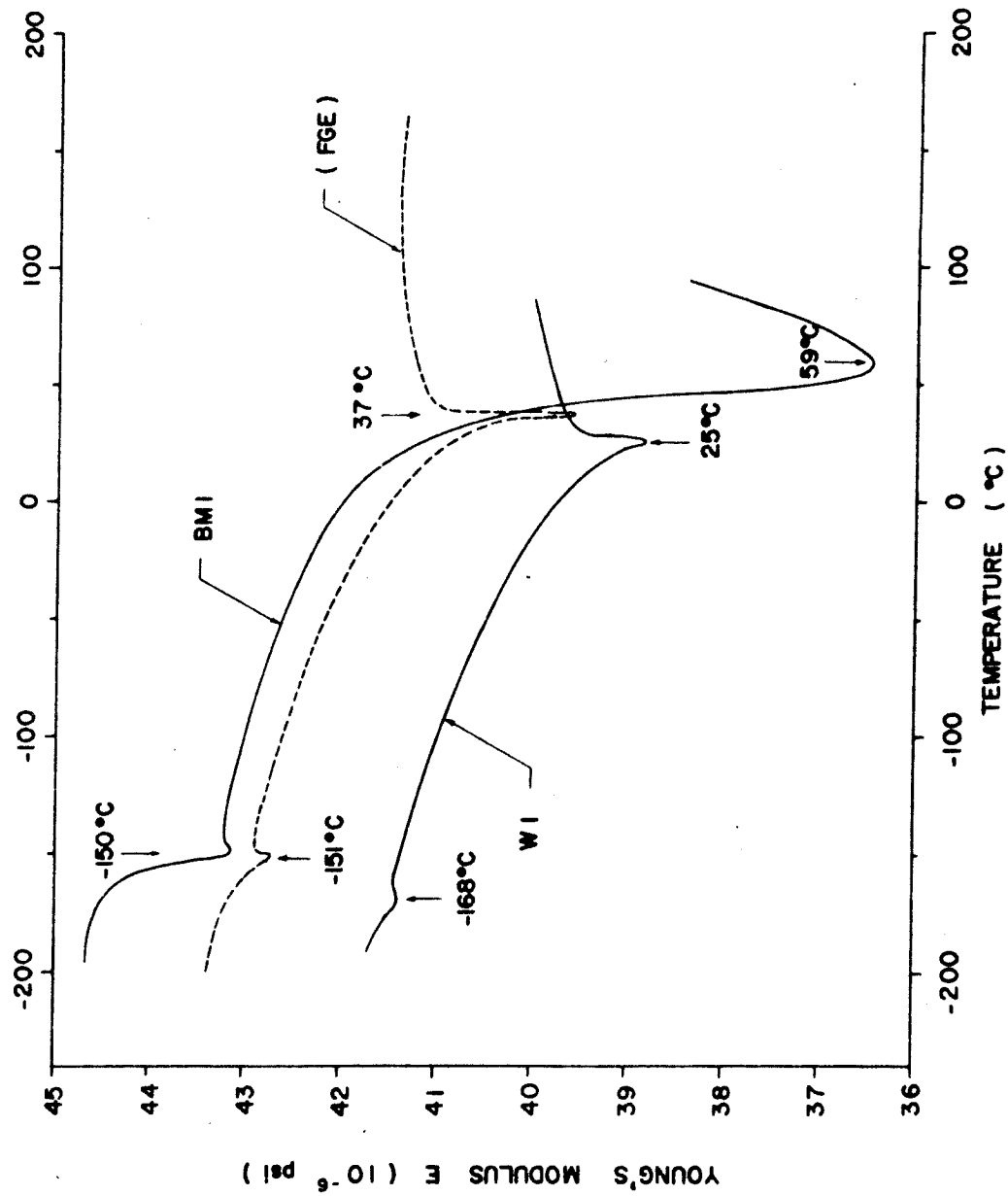

Fig. 14. Young's modulus versus temperature curves for specimens BM 1 and W 1 compared with the results of Fine, Greiner, Ellis (dotted curve).

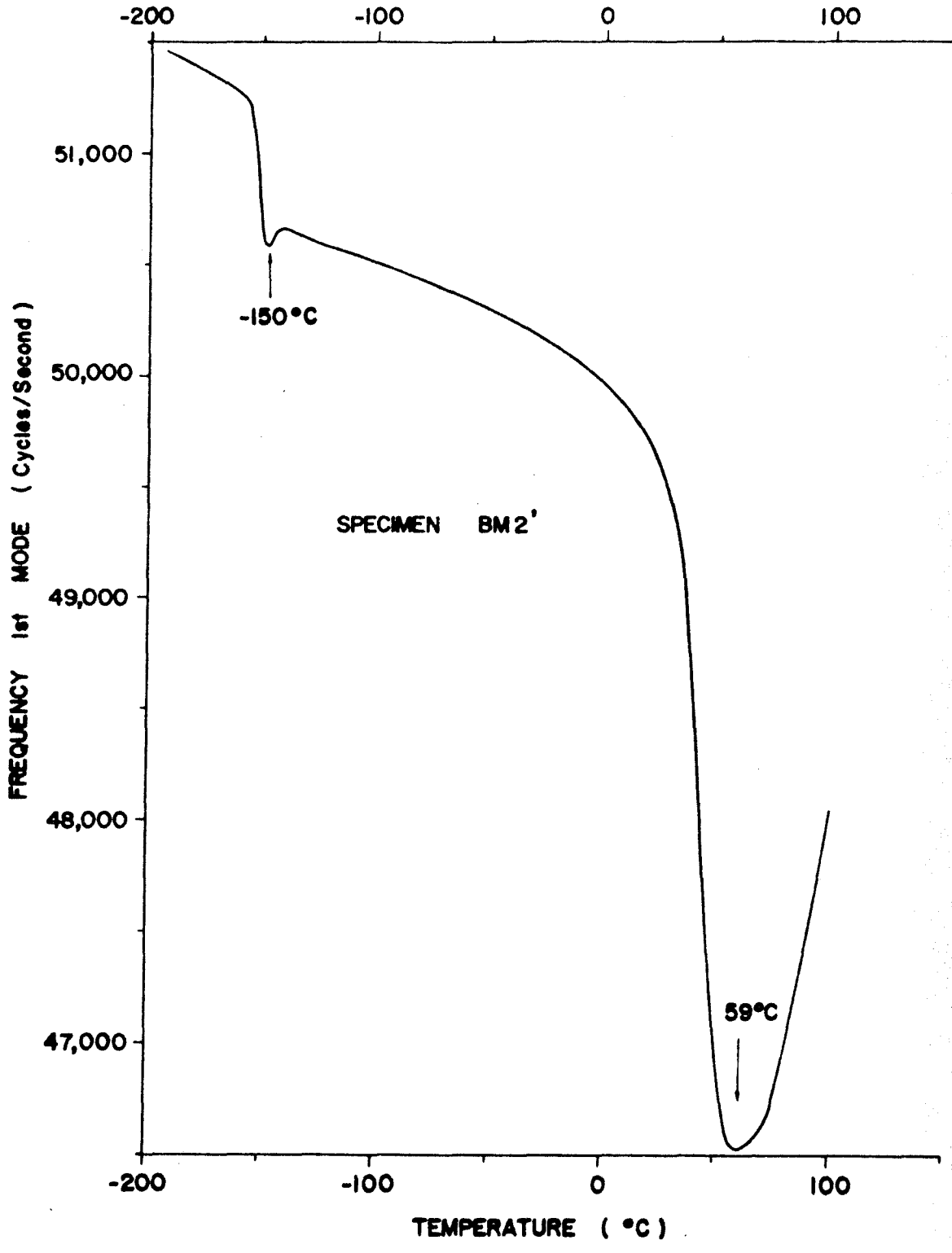

Fig. 15. Frequency of the first mode of vibration versus temperature for specimen BM2'.

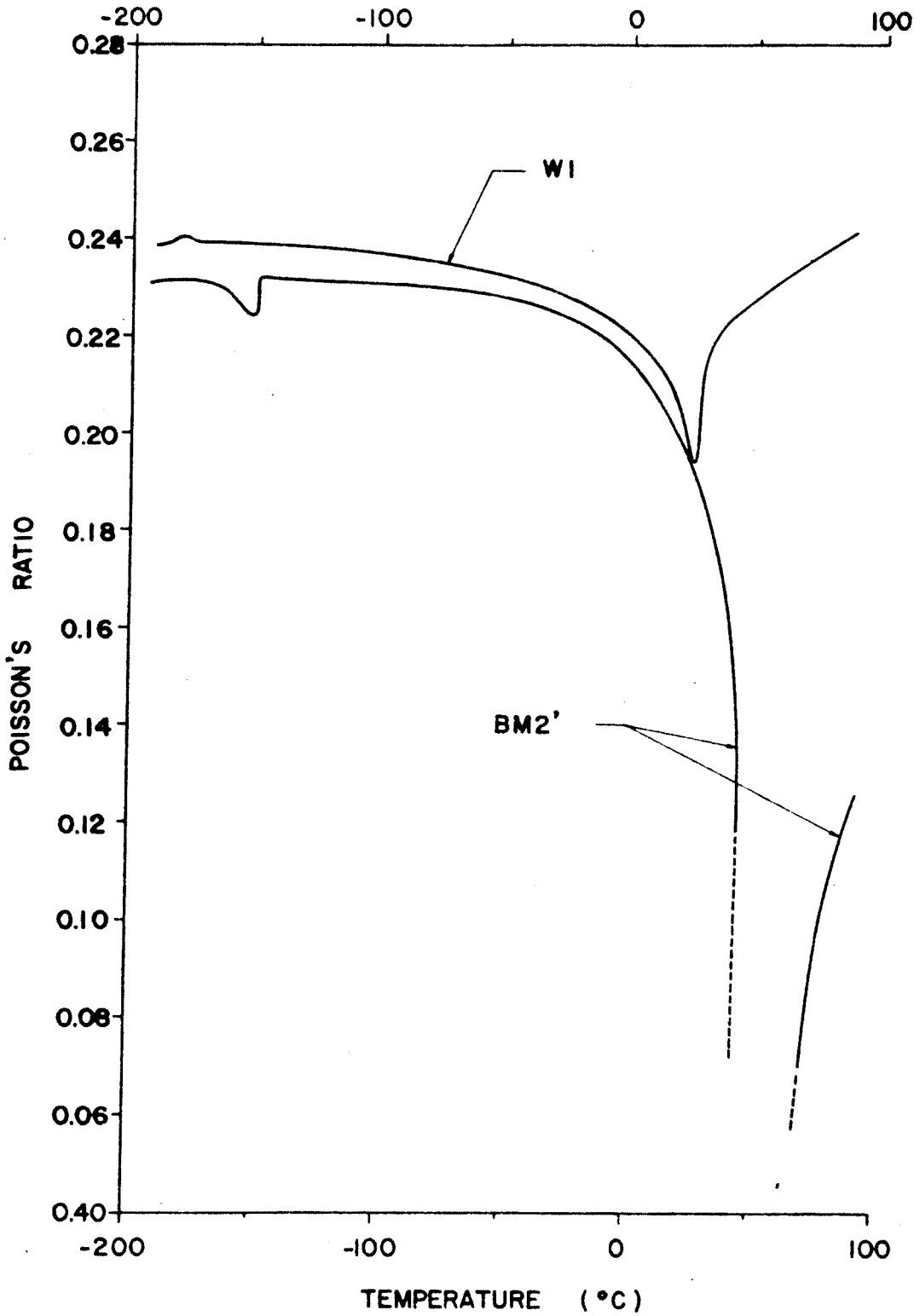

Fig. 16. Poisson's ratio versus temperature curve for specimens W1 and BM2'.

region is shown in Fig. 17 for specimen W1 and in Fig. 18 for specimens BM2 and BM2'. Fig. 17 exhibits an apparent hysteresis, due to a temperature drift of the bath; the effect of annealing appears in Fig. 18, since specimen BM2' is merely specimen BM2 after two hours of annealing at 950 C: it changes only slightly the absolute value of the frequency (i.e., of E) and practically not at all the characteristics of the anomaly.

Finally, the frequency divided by the mode number, versus temperature for various modes, is presented in Fig. 19 and 20 for specimens W1 and BM2' respectively. The curves corresponding to the various modes are not superimposed; the two sets of curves corresponding to the two specimens are very similar, except in the vicinity of the transition above room temperature. The difference between $\frac{1}{n} f_n$ for the first and the eighth mode is of the order of 3% for both specimens outside the transition region; this is larger than expected from Pochhammer treatment: from Rayleigh's equation, the eighth mode ($\frac{a}{\lambda} = 0.20$) corresponds to a value of $\frac{V}{V_o}$ of 0.99 i.e., about 1% difference only with the first mode where $\frac{V}{V_o} \sim 1.0$. In the region of the transition, the dispersion is quite small for specimen BM2', whereas it keeps roughly the same magnitude for specimen W1; as pointed out by Pursey[15], the small value of Poisson's ratio (see Fig. 16) near the transition can account for the absence of dispersion in this range of temperature for specimen BM2', since the velocity of propagation is dependent on Poisson's ratio according to Rayleigh's equation: $\frac{V}{V_o} = 1 - \sigma^2 \pi^2 (\frac{a}{\lambda})^2$.

5.3. HALL COEFFICIENT.

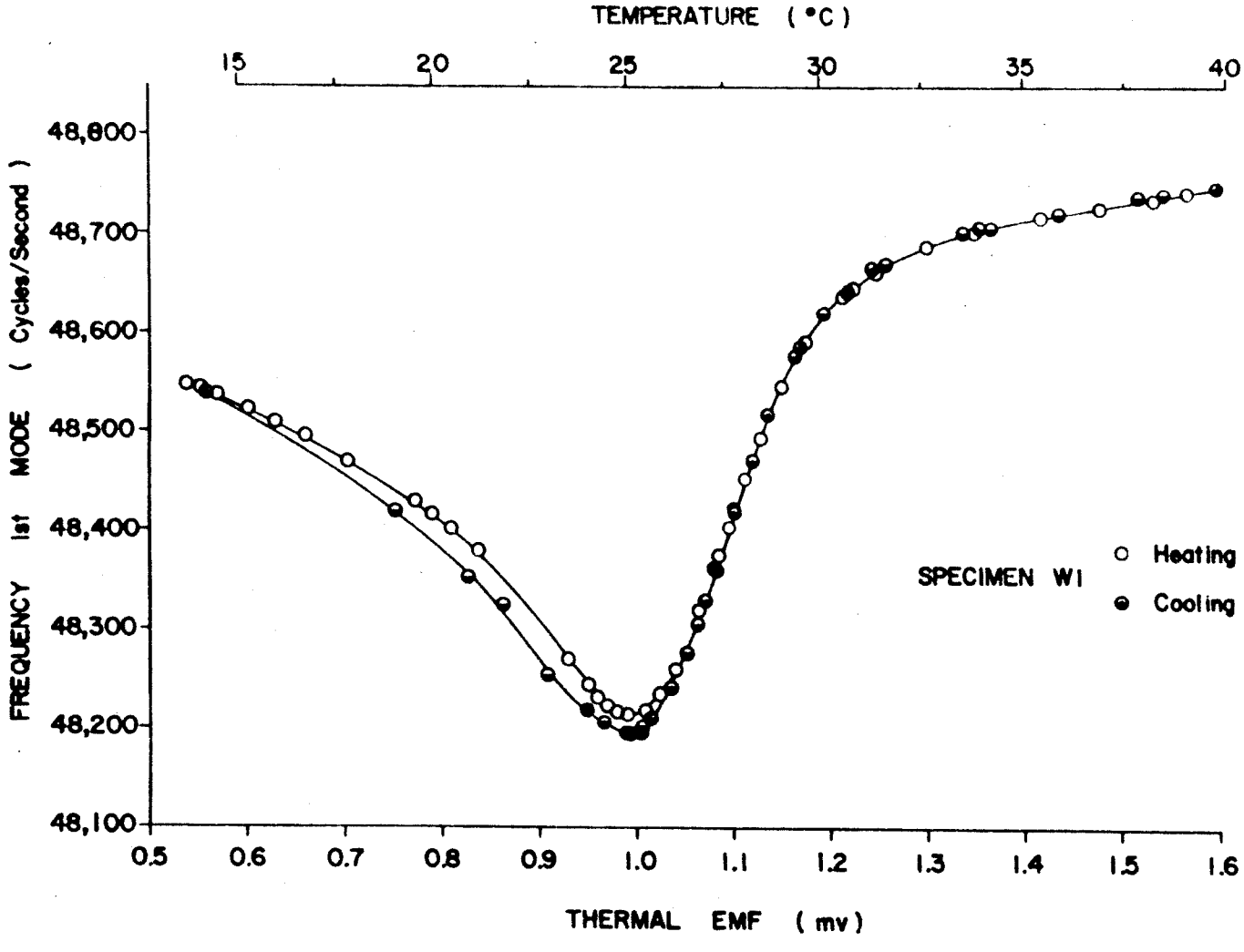

Fig. 17. Frequency of the first mode of vibration versus temperature in the transition region of specimen W1.

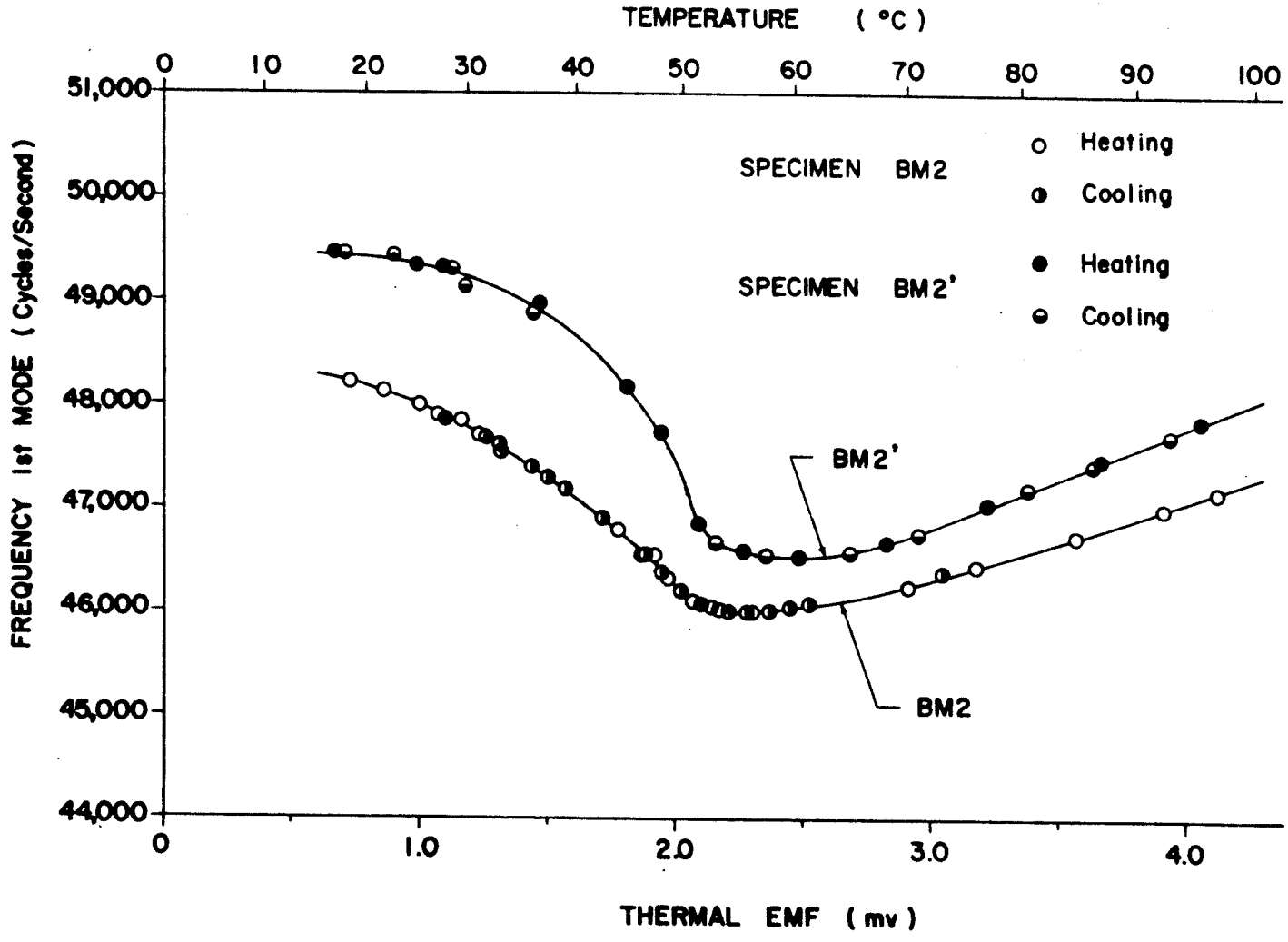

Fig. 18. Frequency of the first mode of vibration versus temperature curve in the transition region of specimens BM2 and BM2'.

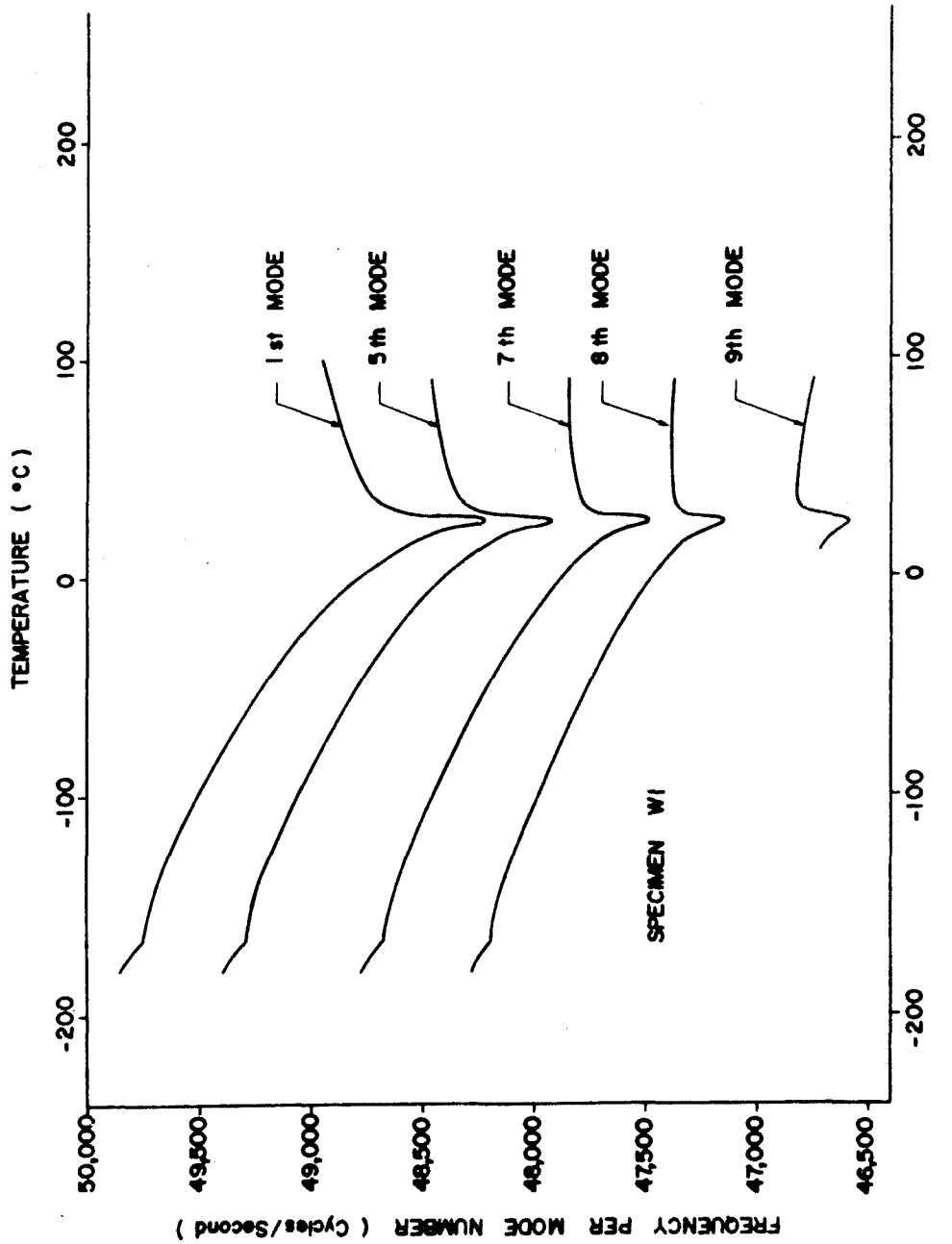

Fig. 19. Frequency per mode number versus temperature curves for various modes of vibration of specimen W1.

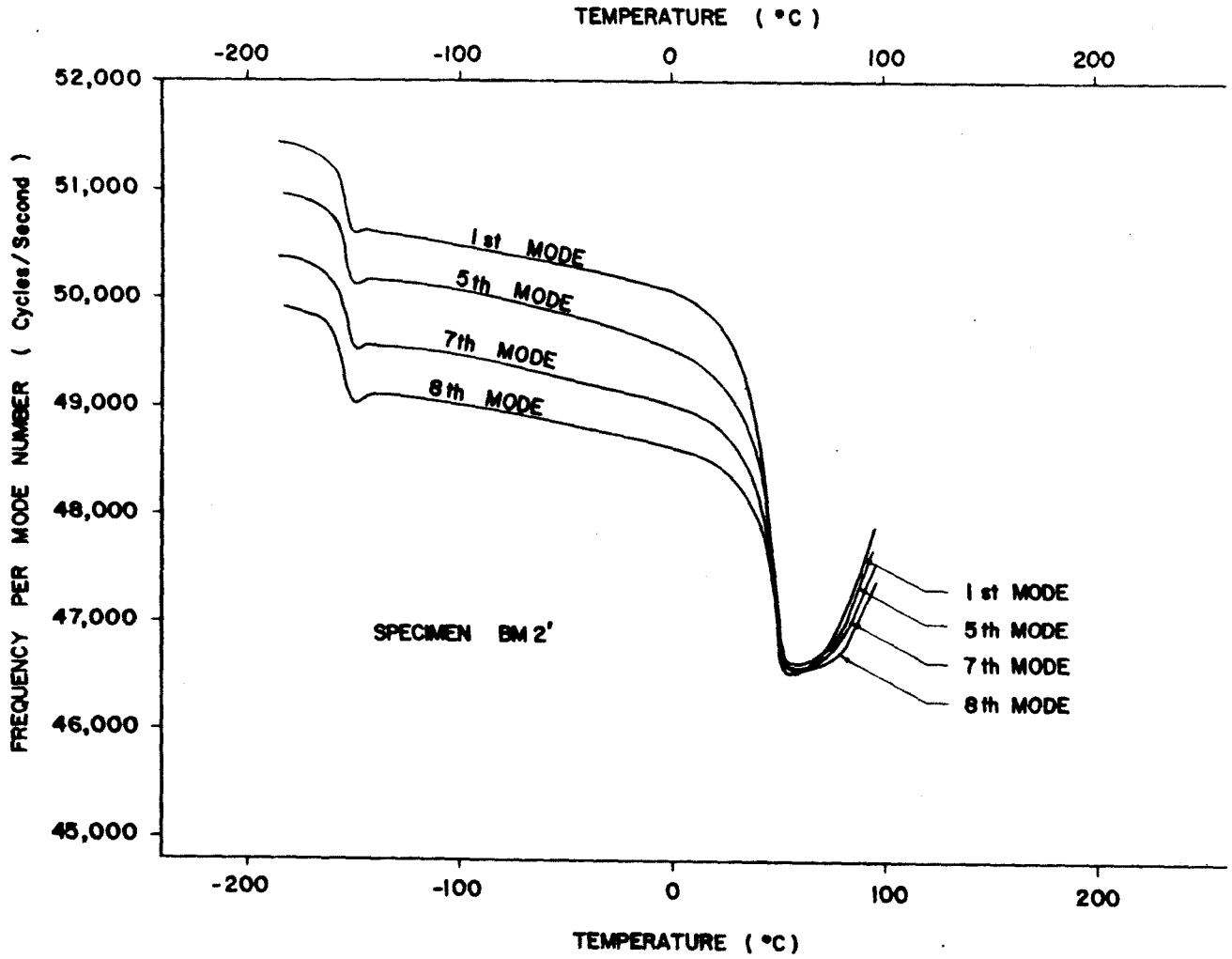

Fig. 20. Frequency per mode number versus temperature curves for various modes of vibration of specimen BM2'.

The variation with temperature of the Hall coefficient R_H for specimens BT and W1 is plotted in Fig. 21 and 22. The values of R_H at room temperature (20C) are estimated to be $+ 34 \pm 2 \times 10^{-13}$ and $+ 28 \pm 3 \times 10^{-13}$ volt.cm/amp. gauss; these values are in fair agreement with the results of Foner [25] which reports $R_H = 36.3 \times 10^{-13}$ volt cm/amp. gauss at 14C. Although the experimental uncertainty is too large to ascertain a very conclusive evidence of an anomaly in the temperature dependence of the Hall coefficient, the experimental data appear to be reasonably well fitted by two portions of a straight line, with slopes - 0.45 and - 0.05 volt. cm/amp. gauss. (C), respectively, in the lower and in the upper temperature region; the discontinuities occur at around 42C for specimen BT and 35C for specimen W1.

5.4. SPECIFIC HEAT.

Typical recordings of T_1 versus ΔT curves during a heating experiment above room temperature are shown in Fig. 23, with an increasing rate of heating from recording I to recording III (respectively 0.12, 0.20, and 0.29 degree C per minute at the temperature of the transition). These recordings show the presence of a flat region at about 36 C corresponding to a variation δT of 0.269 C and 0.193 C respectively for recordings I and II. We can interpret it as a transition during which the temperature T_1 of the chromium specimen remains constant while the temperature T_2 of the copper specimen increases by δT_2 . We can therefore compute the corresponding jump in specific heat by considering the change:

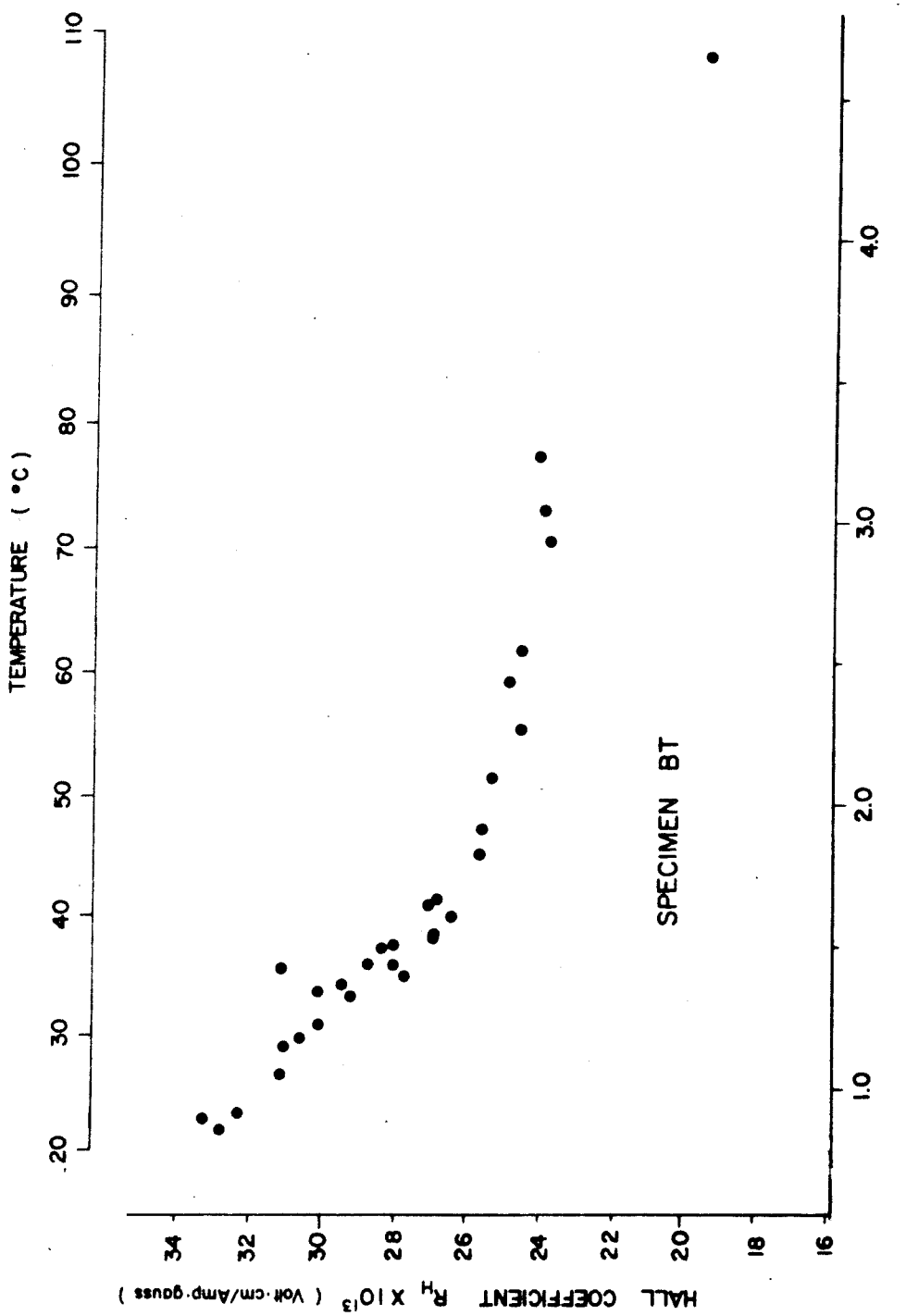

Fig. 21. Hall coefficient versus temperature for specimen BT.

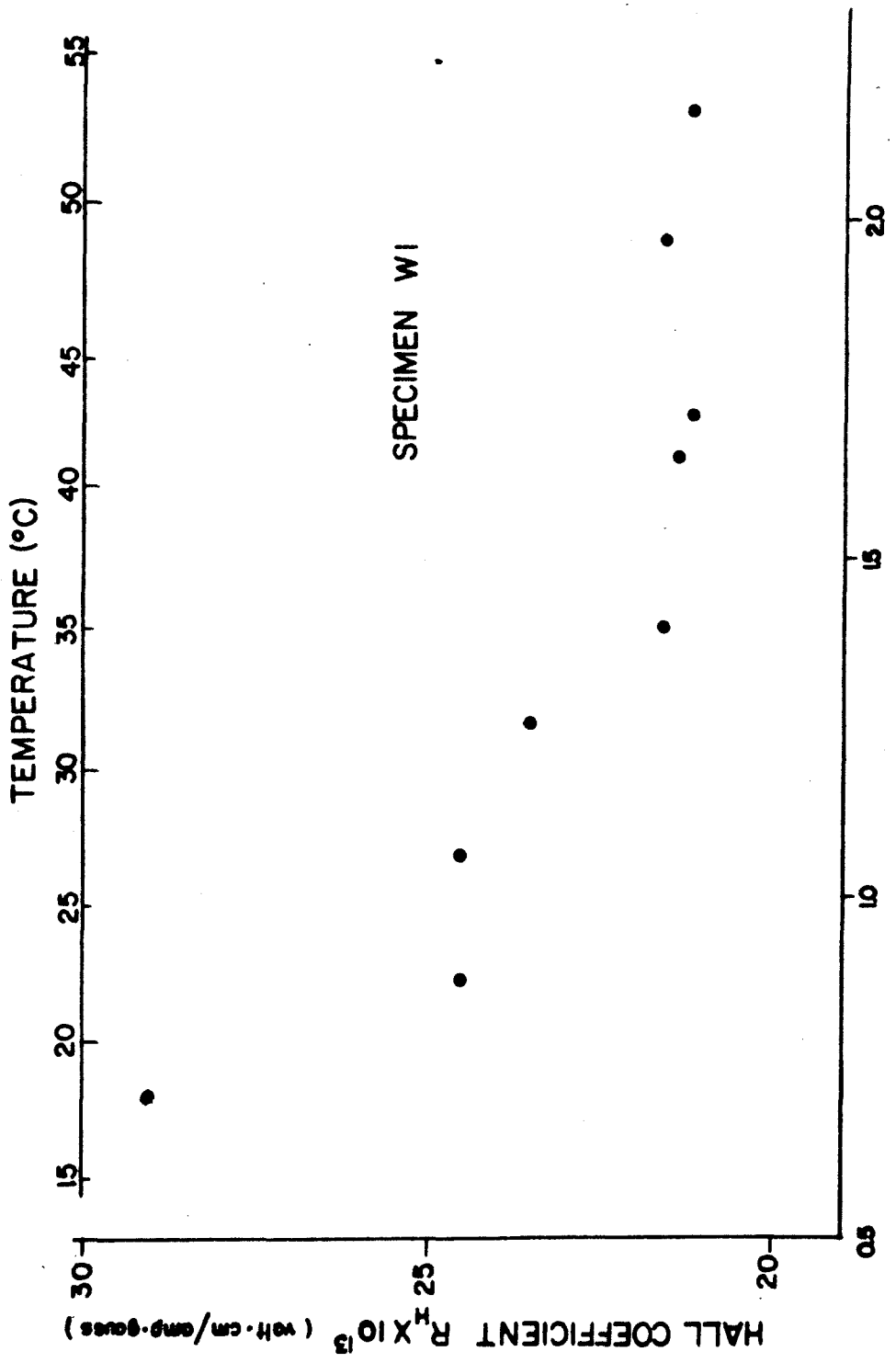

Fig. 22. Hall coefficient versus temperature for specimen W1.

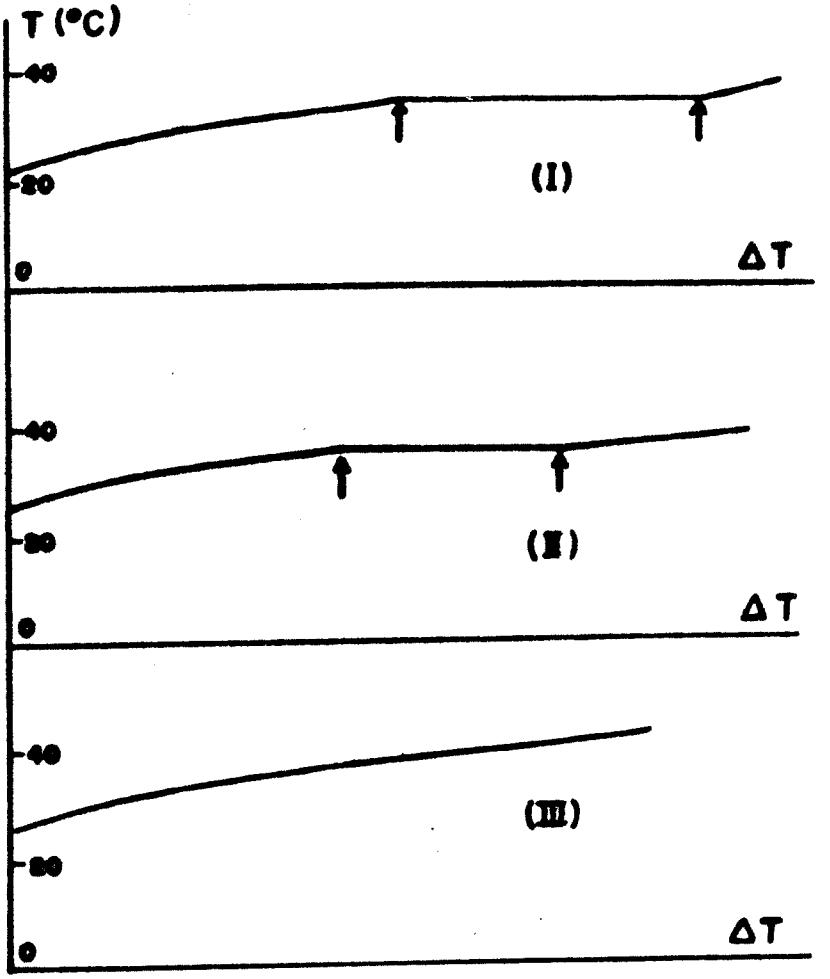

Fig. 23. Typical recordings from specific heat experiments with increasing rates of heating: 0.12 C per minute in recording I, 0.20 C per minute in recording II, 0.29 C per minute in recording III.

$$\delta(\beta_2/\beta_1) = \frac{m_1 C_1}{m_2 C_2} = \frac{\tan^{-1}\left(\frac{x_2+\delta x_2}{a}\right) - \tan^{-1}\left(\frac{x_2}{a}\right) + \frac{1}{2}\ln\frac{(x_2+\delta x_2+a)(x_2-a)}{(x_2+\delta x_2-a)(x_2+a)}}{\tan^{-1}\left(\frac{x_1}{a}\right) - \tan^{-1}\left(\frac{1}{a}\right) + \frac{1}{2}\ln\frac{(x_1+a)(1-a)}{(x_1-a)(1+a)}}$$

All quantities are known here; x_2 and a being very similar and both close to one, δx_2 being small, the Log in the numerator is equivalent to:

$$-\frac{1}{2}\ln\left(1+\frac{\delta x_2/a}{1-x_2/a}\right)$$

From recordings I, II, III, $\frac{\delta C_1}{C_2}$ is equal respectively to 5.2%, 2.8%, and 0.0%, with values of a respectively equal to 1.064, 1.078, and 1.093; extrapolating linearly to an infinitely slow rate of heating through the transition (i.e. a = 1.046), $\frac{\delta C_1}{C_2}$ = 8.5%, i.e., a peak of approximate height 0.48 cal per mole. (deg C) in the specific heat C_1 of chromium. The uncertainty on this last result can be estimated to be about $\pm$ 0.05 and is mainly due to uncertainties in the calculation procedure: the quantity $\delta(\beta_2/\beta_1)$ has a rather sensitive dependence on the difference $(x_2 - a)$ and x_2 and a are both close to one, especially at slow rates of heating; moreover, the extrapolation process to an infinitely slow rate of heating introduces an additional uncertainty.

Finally, the same experiment has been performed with two identical samples of copper, instead of the copper and chromium samples; the same range of temperatures was covered and no such anomaly was found in the T_1 versus ΔT curves.

The only data published on the specific heat of chromium are those of Armstrong and Grayson-Smith[26], which did not show any anomaly; their measurements, however, in the range of temperatures covering the transition, were not close enough to ascertain or to rule out the presence of an anomaly of the order of magnitude of that disclosed in the present work.

VI. DISCUSSION OF RESULTS

The anomalies in the various physical properties of chromium investigated in this thesis are first discussed for their relative correlation in magnitude, shape, and temperature, then interpreted in the light of an explanation of the nature of the transition in chromium.

6.1. COMPARISON OF EXPERIMENTAL RESULTS .

Table II presents the essential features of the observed anomalies and allows a comparison of different properties for a given specimen or of different specimens for a given property.

The low temperature anomaly observed in Young's modulus and Poisson's ratio has not been detected in any other property. In particular, a very careful investigation of the variation of resistance in the critical region of temperature could not disclose any departure from linearity. Although the shape of the anomalies in the E versus temperature curves suggests that both transitions are of similar nature, it should be concluded that for some reason, the low temperature transition affects only the elastic properties of chromium, at the exclusion of the other physical properties investigated. The following discussion will be mostly concerned with the transition above room temperature.

From Table II, it can be seen that the temperatures at which the anomalies occur differ from specimen to specimen. For one given specimen, however, there is a fair correlation between the temperature of the anomalies for various properties. For instance, for specimen W1, where three properties have been investigated, the temperature T_e of the end of the transition derived from each ex-

periment agree within a few degrees.

The magnitude of the anomaly depends on the nature of the specimen and is reflected in the measurements of different properties on a given sample. For example, specimen BM2 exhibits a large anomaly in elastic properties E and σ, and also a large change in slope between the regions of linear variation in the resistivity versus temperature curves (although there is no minimum in the coefficient of resistance). On the other hand, for specimen W1, both the magnitude of the anomaly in E or σ and the change in slope in the resistivity curves are smaller than for specimen BM2.

We can also compare the resistivity and Hall coefficient determinations for specimens W1 and BT. The temperatures at which the break occurs in the slope of the Hall coefficient correspond within a few degrees to the transition temperature T_e deduced from resistivity measurements. It is more difficult, however, to relate the absolute values of resistivity and Hall coefficient, because they are both subject to uncertainties of a few percent, as was pointed out previously in 4.1 and 4.3., and because the mechanism of conduction, to which both properties are directly related is far from being clearly established for chromium. The value R_H of the Hall constant in chromium is positive and relatively large when compared with that of other transition elements closest to chromium in the periodic chart[25]. The hole conduction is therefore the predominant mechanism: the number of holes or their mobility should be large with respect to the number

or the mobility of electrons. Like in the other transition metals, the s and d electron energy bands are assumed to be overlapping: it is also believed that the d-band has a density of states on the average about 20 times larger than the density of the s-band[23]. Consequently, the d-electrons have a large effective mass and their efficiency for conduction is much smaller than that of s-electrons. On the other hand, the Fermi energy in chromium is near the central region of the d-band, where the density of states is believed to be a minimum: the average mobility of the d-electrons is then higher in chromium than in vanadium and manganese. Finally, X-ray scattering experiments[27] show that only a small fraction of the d-electrons remains localized on chromium atoms (0.2 ± 0.4 in chromium, as compared to 2.3 in iron, 8.4 in cobalt, 9.8 in copper): more d-electrons are available for conduction in chromium than in the other transition metals. It is therefore reasonable to assume that: 1/ the large difference in Hall coefficient between chromium and the other transition elements adjacent to it should be ascribed to the role of d-electrons and 2/ the hole predominance is due to d-electrons rather than to s-electrons, as is generally assumed, the latter being on the average closer to the bottom of the d-band.

6.2. POSSIBLE EFFECTS OF IMPURITIES.

As for the large discrepancies in the results concerning the temperature and the shape of the anomalies in resistivity and in Young's modulus between the different specimens used in this study or as reported by other investigators, some recently published works have clearly demonstrated the dependence of the characteristics of the anomaly on the purity of the sample being investigated.

Pursey[15] studied Young's modulus and resistivity of a few samples in which controlled amounts of impurity were added; the effect of four impurities were investigated separately, namely iron (up to 5%), silicon (up to 0.56%), nickel (up to 2%), and copper (up to 1%); in all cases, the effect of the impurity was to depress the temperature of the anomaly (for example, down to -140 C in a 2% Ni specimen) and sometimes to increase greatly the size of the anomaly (particularly in the case of Ni and Si). De Vries[28] investigated the resistivity and Hall effect of samples with small amounts (about 1%) of other transition elements; vanadium was found to shift the temperature of the anomaly down to -50C, and manganese to shift it up to +190C. Similarly, Beck et al.[29] studied the effect of alloying increasing amounts of iron to chromium up to 16%; the anomaly is progressively shifted to lower temperatures and greatly increased in magnitude: for an alloy with 10% Fe, the resistivity is linearly decreasing over a range of temperatures of about 120C. These experiments show how sensitive the anomaly can be to the purity of the specimen under investigation, and that, even for pure chromium, the shape and temperature of the anomaly should be discussed with appropriate caution.

6.3. THE ANTIFERROMAGNETISM OF CHROMIUM .

Recent work in neutron diffraction experiments has brought strong evidence that the anomalies of the various physical properties investigated in this thesis are due to the loss of antiferromagnetism. The Néel temperature of chromium was first

established by Shull and Wilkinson[12] as being around 200 C; in these experiments, chromium powder was investigated by neutron diffraction. Weiss et al[13] confirmed these results with chromium powder, but found a Néel temperature of 35C for a chromium single crystal. Independently, Bykov et al[14] reported a similar result (44 C for single crystals); in their experiment, the intensity of the (100) magnetic ordering reflection, accompanied with a splitting, has a steep growth below 44 C, as expected, but shows also a very sharp drop to a very small value below -115C. At both temperatures, an anomaly in the coefficient of thermal expansion was observed.

While it seems reasonable to consider the transition near 40C as an antiferromagnetic point, the neutron diffraction results brought up new problems. First, there is a large discrepancy between the Néel temperatures of powder and single crystal (or bulk) specimens: this fact can be compared to the existence of two Néel points, one for a powder, and one for a bulk specimen in gold-manganese alloys, which are antiferromagnetic around the composition Au-Mn[30]. In the results of Bykov, it seems also difficult either to reconcile the low temperature anomaly observed in Young's modulus around -150C with the temperature of loss of antiferromagnetism at -115C, or to explain the absence of any anomaly in the physical properties at this temperature, except for the thermal expansivity reported by Bykov. As a matter of fact, the anomalies in the properties of chromium have some similarity with those exhibited by other antiferromagnetics. In

Young's modulus, it is well known that, on cooling through the Curie or the Néel point of a magnetic or an antiferromagnetic material, an external stress induces, in addition to the normal elastic strain of the lattice, another component of strain due to magnetostrictive deformation accompanying the redistribution of the magnetization vectors; while this explains the sharp rise in E above the Néel point in chromium, as it happens also in CoO or in NiO[31] for instance, it does not explain the initial rapid fall in E starting about 30C below the end of the transition. In the resistivity results, the transition region exhibited in chromium and the peculiar decrease of resistivity in most specimens are also found in other metals and alloys. For example, at the Néel temperature, Mn-Cu alloys show a marked decrease in resistivity and an anomaly in Young's modulus. The Néel temperature of α-Mn is around 90 K and there is a slight decrease in resistivity at this temperature. The addition of 1% manganese to chromium[28] resulted in a shift of the anomaly from 40C up to + 190C: a systematic study of the antiferromagnetic transition in a variety of Cr-Mn alloys would therefore certainly be of interest. The magnetic contribution ρ_{Mag} to the resistivity is in general considered to be monotonicly increasing up to the Curie point where it becomes constant, the subsequent increase in the overall resistivity being due only to the lattice resistivity[32,33]. This model, which is in good agreement with experiment for a number of ferro-and antiferro-magnetics, would account for the overall increase in resistivity during heating in the transition region, but not for the above

mentioned decrease observed just before the Néel point. Finally, practically no information is available on the behavior of the Hall coefficient of either ferromagnetics or antiferromagnetics at their Curie point; no anomaly was found, however, in an antiferromagnetic 85% Mn - 15% Cu alloy[28].

Many antiferromagnetic materials, in particular metallic oxides[34,35] show very sharp maxima in their magnetic susceptibility or specific heat. This is not the case in chromium: only the experiments of Lingebach[36] have disclosed a small hump in the magnetic susceptibility of chromium around 36C and the present study has evidenced a narrow peak in specific heat around the same temperature. It should also be pointed out that the expansivity of antiferromagnetic oxides shows a sharp maximum at the Néel temperature corresponding to an anomalous expansion[37], whereas chromium exhibits a minimum in the expansion coefficient, i.e., an anomalous contraction.

Although the anomalies observed in these different materials are similar and seem to be all related to some antiferromagnetic transition, the details of the anomaly for each property remains to be explained. As pointed out by Smart[38], there is a variety of types of antiferromagnetic ordering, depending on the relative magnitude and sign of the interaction coefficients γ_1 and γ_2 between first neighbors and second nearest neighbors, giving rise to different magnetic lattices. Only additional neutron diffraction experiments can possibly give a more detailed information about the type of interaction due to magnetic forces and

therefore the type of phenomenon to be expected in the course of an antiferromagnetic transition.

VII. CONCLUSION

Anomalies have been observed in four physical properties of chromium investigated in this thesis. Although an interpretation in terms of the loss of antiferromagnetic structure allows to explain qualitatively some of the features of these anomalies, chromium presents some peculiarities not exhibited by other antiferromagnetics: in particular, the large anomalies in resistivity and Young's modulus have no such counterpart in specific heat and magnetic susceptibility, as is the usual case for anitferromagnetics. In addition, a second and still unexplained transition occurs around -150C which is detected by anomalies in the elastic constants only.

The relationship between the loss of antiferromagnetism and the anomalies in various physical properties at the Néel point is not yet clearly established; but before this can be done, additional neutron diffraction experiments are needed to remove or explain the inconsistent results obtained so far.

APPENDIX

The frequency equation reads:

$$\left| A\left[2\mu\frac{\partial^2}{\partial r^2}J_o(h'r)\right|_{r=a} - \frac{\lambda}{\lambda+2\mu}p^2\rho\,J_o(h'a)\right] + 2C\mu\gamma\frac{\partial}{\partial r}J_1(k'r)\Big|_{r=a} = 0 \qquad (1)$$

$$\left| 2A\gamma\frac{\partial}{\partial r}J_o(h'r)\right|_{r=a} + C\left(2\gamma^2 - \frac{p^2\rho}{\mu}\right)J_1(k'a) = 0 \qquad (1)'$$

For brevity, we shall write: $\frac{\partial(\ )}{\partial a}$ for $\frac{\partial(\ )}{\partial r}\Big|_{r=a}$

On the other hand: $\frac{\partial}{\partial a} = h'\frac{\partial}{\partial(h'a)}$ and $\frac{\partial^2}{\partial a^2} = h'^2\frac{\partial^2}{\partial^2(h'a)}$

and the classical relations between Bessel functions and their derivatives read:

$$J_o' = -J_1$$

$$J_o'' + \frac{1}{x}J_o' + J_o = 0$$

$$J_1' = J_o - \frac{1}{x}J_1$$

Finally, we can express h'^2 and k'^2 in terms of x, β, γ :

$$h'^2 = \gamma^2\left[\frac{\rho p^2(1+\sigma)(1-2\sigma)}{\gamma^2 E(1-\sigma)} - 1\right] = \gamma^2(\beta x - 1)$$

$$k'^2 = \gamma^2\left[\frac{2\rho p^2(1+\sigma)}{\gamma^2 E} - 1\right] = \gamma^2(2x - 1)$$

and Lame's coefficients in terms of E, σ :

$$\lambda = \frac{\sigma E}{(1+\sigma)(1-2\sigma)} \quad , \quad \mu = \frac{E}{2(1+\sigma)} \ .$$

The first equation reads after these substitutions:

$$A\left[2\mu\gamma^2(\beta x-1)J_o''(h'a) - \mu\frac{2(1-\beta)}{\beta}\beta x\gamma^2 J_o(h'a)\right] + 2C\mu\gamma k'J_1'(k'a)=0$$

or:

$$A\left[\gamma(\beta x-1)\left\{\frac{J_1(h'a)}{h'a} - J_o(h'a)\right\} - (1-\beta)x\gamma J_o(h'a)\right] + Ck'\left[J_o(k'a) - \frac{1}{k'a}J_1(k'a)\right] = 0 \qquad (2)$$

The same substitutions on the second equation lead to:

$$2A\left[\gamma h'J_o'(h'a)\right] + C\,2\gamma^2(1-x)\,J_1(k'a) = 0$$

or:

$$-Ah'\,J_1(h'a) + C\gamma(1-x)\,J_1(k'a) = 0 \qquad (2)'$$

We introduce then the function $\varphi(y) = \dfrac{y\,J_o(y)}{J_1(y)}$ in the equations (2) and (2)' to get:

$$\left|\begin{array}{ll} A\gamma J_o(h'a)\left[(\beta x-1)\left(\dfrac{1}{\varphi(h'a)} - 1\right) - (1-\beta)x\right] - Ck'J_o(k'a)\left(\dfrac{1}{\varphi(k'a)} - 1\right) = 0 & (3) \\ A\gamma(\beta x-1)\dfrac{J_o(h'a)}{\varphi(h'a)} - C(1-x)k'\dfrac{J_o(k'a)}{\varphi(k'a)} = 0 & (3)' \end{array}\right.$$

In the development of the determinant of the system, we eliminate the trivial solution: $\gamma k'J_o(h'a)J_o(k'a) = 0$ and keep:

$$\frac{(1-x)}{\varphi(k'a)}\left[(x-1) - \frac{\beta x-1}{\varphi(h'a)}\right] + \frac{\beta x-1}{\varphi(h'a)}\left(\frac{1}{\varphi(k'a)} - 1\right) = 0$$

or:

$$(1-x)^2\varphi(h'a) - (\beta x-1)\left[x - \varphi(k'a)\right] = 0$$

REFERENCES

(1) Bridgman, P.W. : "Pressure Coefficients of Resistance of Elements", Proc. Amer. Acad. Art.Sci., Vol.68 (1933),p.32-39.

(2) Söchtig, H. : "Untersuchungen an Reinem Chrom im Anomaliegebiet", Annalen der Physik, Vol.38 (1940), p. 97-120.

(3) Potter, H.H. : "Electrical Resistance and Thermoelectric Power of the Transition Metals", Proc. Phys. Soc. London, Vol.53 (1941), p. 695-705.

(4) Erfling, H.D. : "Studien zur Thermischen Ausdehnung Fester Stoffe in Tiefer Temperatur", Annalen der Physik, Vol.34 (1939), p. 136-160.

(5) Hidnert, P. : "Thermal Expansion of Cast and of Swaged Chromium", U.S. Bur. of Standards, Journal of Research, Vol.27 (1941), p. 113-124.

(6) Bates, L.F., and A. Baqi : "Magnetic Properties of Chromium", Proc. Phys. Soc. London, Vol.48 (1936), p. 781-794.

(7) MacGuire, T.R., and C.J. Kriessman : "The Magnetic Susceptibility of Chromium", Phys. Rev., Vol.85, No. 3, (1952), p.452-454.

(8) Fine, M.E., E.S. Greiner and W. C. Ellis : "Transitions in Chromium", J. of Metals, Vol. 191, No. 1, (1951), p. 56-58.

(9) Pursey, H. : "Thermal Dependence of Elastic Constants of Electrodeposited Chromium", Nature, Vol. 169 (1952), p. 150.

(10) Pursey, H.:"Thermal Anomaly in the Elastic Constants of Chromium", Nature, Vol. 172, (1953), p. 864.

(11) Straumanis, M.E. and C.C. Weng : "The Precise Lattice Constant and the Expansion Coefficient of Chromium between + 10 C and 60 C", Acta Cryst., Vol. 8 (1955), p. 367-371.

(12) Shull, C.G. and M.K. Wilkinson : "Neutron Diffraction Studies of Various Transition Elements", Rev. Mod. Phys. Vol. 25, No. 1 (1953), p. 100-107.

(13) Weiss, R.J., L.M. Corliss and J.M. Hastings : "Antiphase Antiferromagnetic Structure of Chromium", Phys. Rev. Lett., Vol. 3 (1959), p. 211.

(14) Bykov et al. : "Magnetic Properties of Chromium", Soviet Physics Dokladi, (Translation), Vol. 4, No. 5 (1960), p. 1070-1073.

(15) Pursey, H. : "A New Investigation of Anomalies in Chromium", Journ. Inst. Met., Vol. 86 (8), (1957), p. 362-368.

(16) Kolsky, H. : "Stress Waves in Solids", Chap. III, Oxf. at Clarendon Press (1953).

(17) Onoe, M. : "Modified Quotients of Bessel Functions", Columbia University Press, (1958).

(18) Bancroft, D. : "The Velocity of Longitudinal Waves in Cylindrical Bars", Phys. Rev., Vol. 59 (1941), p. 588-593.

(19) Mott, N.F. and H. Jones : "The Theory of the Properties of Metals and Alloys", Dover Publ. Inc., New York (1958).

(20) Kapitza, P. : "The Change of Electrical Conductivity in Strong Magnetic Fields", Proc. Roy. Soc. London, Vol. 123 A (1929), p. 292-372.

(21) Denney, J.M., : "A Study of Electron Effects in Solid Solutions Alloys of Titanium", PhD Thesis (1954), California Institute.

(22) MacAdams, W.H. : "Heat Transmission", MacGraw-Hill (1954).

(23) Slater, J.C. : "Introduction to Chemical Physics", MacGraw-Hill (1939).

(24) Kittel, C. : "Introduction to Solid State Physics", John Wiley & Sons (1953).

(25) Foner, S. : "Hall Effect in Titanium, Vanadium, Chromium and Manganese", Phys. Rev., Vol. 107, No. 6 (1957), p. 1513-1516.

(26) Armstrong, L.D. and H. Grayson-Smith : "High Temperature Calorimetry : Atomic Heats of Chromium, Manganese and Cobalt between 0 C and 800 C", Can. Journ. Res., Vol. 28A (1950), p. 51-59.

(27) Weiss, R.J., and J.J. De Marco : "X-Ray Determination of the Number of 3 d-electrons in Cu,Ni,Co,Fe, and Cr", Rev. Mod. Phys., Vol. 30 (1958), p. 59-62.

(28) De Vries, G. : "The Transition in Chromium and in Some Alloys of Chromium with Small Amounts of Other Transition Elements", J. Phys. Rad., Vol. 20 (1959), p. 438-439.

(29) Beck, P.A., N.S. Rajan and R.M. Waterstrat : "Temperature Dependence of the Electrical Resistivity of bcc Cr-Fe Alloys", J. Appl. Phys., Vol. 31, No. 4 (1960), p. 731-732.

(30) Giansoldati, A., J.O. Linde and G. Borelius : "The Anti-ferromagnetic Transformation of the Alloy Au-Mn", J. Phys. Chem. Sol., Vol. 9 (1959), p. 183-184.

(31) Street, R., and B. Lewis : "Anomalous Variation of Young's Modulus of Antiferromagnetics at the Néel Point", Nature, Vol. 168 (1951), p. 1036-1037.

(32) Fridel, J. and P. De Gennes : "Anomalies de Résistivité dans Certains Métaux Magnétiques", J. Phys. Chem. Sol., Vol. 4 (1958), p. 71-77.

(33) Weiss, R.J. and A.S. Marotta : "Spin Dependence of the Resistivity of Magnetic Metals," J. Phys. Chem. Sol. Vol. 9 (1959), p. 302-308.

(34) Bizette, H., C.F. Squire and B. Tsai : "Le Point de Transition λ de la Susceptibilité Magnétique du Protoxyde de Manganèse Mno", Compt. Rend.,Vol. 207 (1938), p. 449-450.

(35) Millar, R.W. : "The Specific Heat at Low Temperatures of Manganous Oxide, Manganous-Manganic Oxide and Manganese Dioxide", J. Amer. Chem. Soc., Vol. 50 (1928), p. 1875-1883.

(36) Lingelbach, R. : "Magnetische Untersuchungen an Chrom und Chrom Mischkristallen", Z. Physical.Chem. Vol. 14 (1958), p. 1-31.

(37) Föex, M. : "Sur un Type de Transformation Commun aux Protoxydes de Manganèse, Fer, Cobalt et Nickel", Compt. Rend., Vol. 227 (1948), p. 193-194.

(38) Smart, J.S. : "The Molecular Field Treatment of Anti-ferromagnetism", Rev. Mod. Phys., Vol. 25, No. 1 (1953), p. 327-331.